

2

DTIC E. COPY

TECHNICAL REPORT HL-89-15

# PROTOTYPE EVALUATION OF BAY SPRINGS LOCK TENNESSEE-TOMBIGBEE WATERWAY, MISSISSIPPI

by

Richard G. McGee

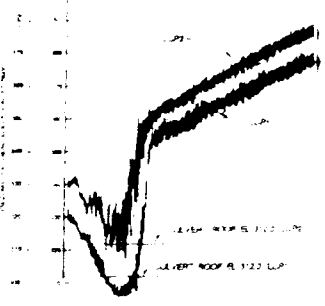
Hydraulics Laboratory

DEPARTMENT OF THE ARMY  
Waterways Experiment Station, Corps of Engineers  
PO Box 631, Vicksburg, Mississippi 39181-0631



US Army Corps  
of Engineers

AD-A212 431



August 1989  
Final Report

Approved For Public Release; Distribution Unlimited

**DTIC**  
**ELECTE**  
**SEP 19 1989**  
**S B D**



Prepared for US Army Engineer District, Mobile  
Mobile, Alabama 36628-0001

89 9 18 16 0

Destroy this report when no longer needed. Do not return  
to the originator.

The findings in this report are not to be construed as an official  
Department of the Army position unless so designated  
by other authorized documents.

The contents of this report are not to be used for  
advertising, publication, or promotional purposes.  
Citation of trade names does not constitute an  
official endorsement or approval of the use of  
such commercial products.

Unclassified

SECURITY CLASSIFICATION OF THIS PAGE

REPORT DOCUMENTATION PAGE				Form Approved OMB No 0704-0188	
1a REPORT SECURITY CLASSIFICATION Unclassified		1b RESTRICTIVE MARKINGS			
2a SECURITY CLASSIFICATION AUTHORITY		3 DISTRIBUTION AVAILABILITY OF REPORT Approved for public release; distribution unlimited.			
2b DECLASSIFICATION/DOWNGRADING SCHEDULE					
4 PERFORMING ORGANIZATION REPORT NUMBER(S) Technical Report HL-89-15		5 MONITORING ORGANIZATION REPORT NUMBER(S)			
6a NAME OF PERFORMING ORGANIZATION USAEWES Hydraulics Laboratory	6b OFFICE SYMBOL (If applicable) CEWES-HS-H	7a NAME OF MONITORING ORGANIZATION			
6c ADDRESS (City, State, and ZIP Code) PO Box 631 Vicksburg, MS 39181-0631		7b ADDRESS (City, State, and ZIP Code)			
8a NAME OF FUNDING/SPONSORING ORGANIZATION USAEB, Mobile	8b OFFICE SYMBOL (If applicable)	9 PROCUREMENT INSTRUMENT IDENTIFICATION NUMBER			
8c ADDRESS (City, State, and ZIP Code) PO Box 2288 Mobile, AL 36628-0001		10 SOURCE OF FUNDING NUMBERS			
		PROGRAM ELEMENT NO	PROJECT NO	TASK NO	WORK UNIT ACCESSION NO
11 TITLE (Include Security Classification) Prototype Evaluation of Bay Springs Lock, Tennessee-Tombigbee Waterway, Mississippi					
12 PERSONAL AUTHOR(S) McCee, Richard G.					
13a TYPE OF REPORT Final report	13b TIME COVERED FROM _____ TO _____	14 DATE OF REPORT (Year, Month, Day) August 1989		15 PAGE COUNT 86	
16 SUPPLEMENTARY NOTATION Available from National Technical Information Service, 5285 Port Royal Road, Springfield, VA 22161.					
17 COSATI CODES		18 SUBJECT TERMS (Continue on reverse if necessary and identify by block number)			
FIELD	GROUP				
			Bay Springs Lock Navigation		
			Cavitation Prototype tests		
			Locks (waterways) Venting (air demand)		
19 ABSTRACT (Continue on reverse if necessary and identify by block number)					
<p>Prototype tests were conducted to comprehensively evaluate the performance of the 84-ft-lift Bay Springs Lock, located at the southern end of the Divide Section of the Tennessee-Tombigbee Waterway. The evaluation included analysis of the operating characteristics and hydraulic efficiency of the lock as well as a comparison of the physical and analytical model results with the prototype. Prototype measurements included pressures in the culvert system, air vent flow rates, downstream approach canal surges, valve movement and cylinder pressures, and water-surface elevations.</p> <p>Results indicate that satisfactory operating conditions exist at Bay Springs Lock. The lock has functioned without major operational problems and the prototype test data do not indicate any area in which major operational problems might be expected. Air venting just downstream of all valves is required to eliminate large-scale cavitation. Small</p> <p style="text-align: right;">(Continued)</p>					
20 DISTRIBUTION/AVAILABILITY OF ABSTRACT <input checked="" type="checkbox"/> UNCLASSIFIED/UNLIMITED <input type="checkbox"/> SAME AS RPT <input type="checkbox"/> DTIC USERS		21 ABSTRACT SECURITY CLASSIFICATION Unclassified			
22a NAME OF RESPONSIBLE INDIVIDUAL		22b TELEPHONE (Include Area Code)		22c OFFICE SYMBOL	

19. ABSTRACT (Continued).

cavitation occurs following the vented periods; however, the time duration is so short that the design is acceptable. The 6-in. orifices installed on the filling valve air intakes for controlling air entrainment seemed to be the optimum size. Venting without the intake orifice installed (12-in.-diam opening) resulted in unacceptable chamber water-surface conditions due to the large amount of air entrained in the flow. Without venting, severe cavitation occurred. A 4-ft surge was generated in the downstream canal during normal emptying operations.

Comparison of the prototype with the previous physical model studies and an analytical model showed reasonable agreement between predicted conditions and actual conditions. As expected, the physical model was less efficient than the prototype. Predictions of critical culvert pressures (below the valves) were higher than those measured in the prototype. The analytical model, when calibrated with operation time, more closely predicted these critical pressures. Prototype values for surge height were higher than the results for both the physical and analytical models.

PREFACE

The prototype tests described herein were conducted during August 1985 by the US Army Engineer Waterways Experiment Station (WES) under the sponsorship of the US Army Engineer District, Mobile.

The overall test program was conducted under the general supervision of Messrs. F. A. Herrmann, Jr., Chief of the Hydraulics Laboratory; M. B. Boyd, Chief of the Hydraulic Analysis Division; and G. A. Pickering, Chief of the Hydraulic Structures Division. Mr. R. G. McGee, Hydraulic Analysis Branch, was the test coordinator. This report was prepared by Mr. McGee under the supervision of Messrs. E. D. Hart, Chief of the Prototype Evaluation Branch, and Dr. B. J. Brown, Chief of the Hydraulic Analysis Branch, and edited by Mrs. Marsha Gay, Information Products Division, WES. Instrumentation support was provided by Mr. S. W. Guy and Mr. M. Jones under the supervision of Mr. L. M. Duke, Chief of the Operations Branch, Instrumentation Services Division, WES. Additional assistance in the investigation was provided by Dr. F. M. Neilson of the Hydraulic Engineering Information Analysis Center (HEIAC), Hydraulics Laboratory.

Acknowledgment is made to the personnel of the Mobile District and the US Army Diving Attachment, Fort Eustis, VA, for their assistance in the investigation.

Acting Commander and Director of WES during preparation of this report was LTC Jack R. Stephens, EN. Technical Director was Dr. Robert W. Whalin.

Accession For	
NTIS GRA&I	<input checked="" type="checkbox"/>
DTIC TAB	<input type="checkbox"/>
Unannounced	<input type="checkbox"/>
Justification	
By	
Distribution/	
Availability Codes	
Dist	Avail and/or Special
A-1	

## CONTENTS

	<u>Page</u>
PREFACE.....	1
CONVERSION FACTORS, NON-SI TO SI (METRIC) UNITS OF MEASUREMENT.....	3
PART I: INTRODUCTION.....	5
Pertinent Features of the Project.....	5
Purpose and Scope of the Study.....	7
Prior Model Studies.....	7
PART II: MEASUREMENTS, EQUIPMENT, AND PROCEDURES.....	8
Measurements and Equipment.....	8
Recording Equipment.....	12
Testing Procedure and Conditions.....	12
Recording Procedures.....	15
Analysis Procedures.....	16
PART III: BASIC LOCK PERFORMANCE.....	17
Lock Performance Parameters.....	17
Valve Operation.....	17
Valve Hoist Loads.....	19
Filling and Emptying.....	21
PART IV: HYDRAULIC CHARACTERISTICS OF THE CULVERTS AND VALVES.....	39
Culvert Pressures Downstream from Valves.....	39
Valve Well Water-Surface Elevations.....	41
Valve Discharge and Contraction Coefficients.....	42
Cavitation Index.....	44
PART V: CONCLUSIONS AND RECOMMENDATIONS.....	46
Basic Lock Performance.....	46
Hydraulic Characteristics.....	47
Culvert Pressures.....	47
Effects of Air Venting on Culvert Pressure.....	47
Cavitation.....	48
Model-Prototype Comparisons.....	48
Instrumentation Facilities.....	49
REFERENCES.....	51
TABLES 1-8	
PLATES 1-20	
APPENDIX A: NOTATION.....	A1

CONVERSION FACTORS, NON-SI TO SI (METRIC) UNITS OF MEASUREMENT

Non-SI units of measurement used in this report can be converted to SI (metric) units as follows:

<u>Multiply</u>	<u>By</u>	<u>To Obtain</u>
acre-feet	1,233.489	cubic metres
acres	4,046.873	square metres
cubic feet	0.02831685	cubic metres per second
degrees (angle)	0.1745329	radians
degrees Fahrenheit	5/9	Celsius degrees or Kelvins*
feet	0.3048	metres
inches	2.54	centimetres
kips (force)	4.448222	kilonewtons
miles (US statute)	1.609344	kilometres
pounds (mass) per cubic foot	16.01846	kilograms per cubic metre
pounds (mass) per cubic inch	27.6799	grams per cubic centimetre
pounds (force) per square inch	6,894.757	pascals
square feet	0.09290304	square metres

---

\* To obtain Celsius (C) temperature readings from Fahrenheit (F) readings, use the following formula:  $C = (5/9)(F - 32)$ . To obtain Kelvin (K) readings, use:  $K = (5/9)(F - 32) + 273.15$ .

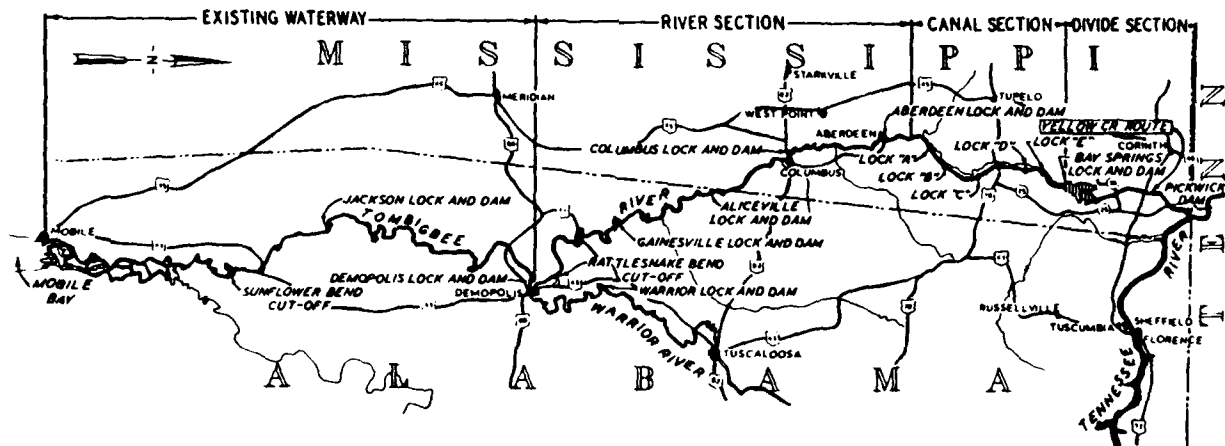


Figure 1. Vicinity and location map

PROTOTYPE EVALUATION OF BAY SPRINGS LOCK,  
TENNESSEE-TOMBIGBEE WATERWAY, MISSISSIPPI

PART: INTRODUCTION

Pertinent Features of the Project

1. Bay Springs Lock and Dam, located in the southwest corner of Tishomingo County, Mississippi (Figure 1), is the uppermost navigation structure on the Tennessee-Tombigbee Waterway. It is located at the southern end of the Divide Section of the waterway, creating a pool extending through the Divide Cut to Pickwick Lake and the Tennessee River.

2. The existing project (Figure 2) consists of a 2,800-ft\* rock-fill dam, navigation lock, downstream channel, and lake. Bay Springs Lake has a normal summer pool at el 414\*\* and is designed for a maximum pool elevation of 422. At normal pool the lake has a surface area of 6,700 acres and 180,000 acre-feet of storage. The downstream canal, excavated in rock with side slopes of 4V on 1H for a distance of approximately 1 mile, has a base width of 300 ft and a depth of 13 ft with the normal water surface (el 330). This elevation is provided by Lock and Dam E located 5.2 miles downstream.

3. The lock, located near the left end of the dam and perpendicular to the axis of the dam, has nominal chamber dimensions of 110 ft wide by 600 ft long with 670 ft between center lines of the miter gate pintles. It has a lift of 84 ft at normal upper and lower pool levels. The upper sill is at el 390 and the lower sill at el 315. Each sill acts as the seal for the respective miter gate. The minimum clearance is 18 ft for the upper sill and 15 ft for the lower sill. Pertinent details of the lock design are shown in Plate 1. The filling and emptying system consists of 10-port intake manifolds located in the chamber side of each lock wall immediately upstream of the miter gate sill; 14- by 14-ft longitudinal culverts in each lock wall; filling and emptying valves of the same size as the culverts; a crossover culvert with a horizontal splitter plate in each main culvert to divide flows into each

---

\* A table of factors for converting non-SI units of measurement to SI (metric) units is presented on page 3.

\*\* All elevations (el) cited herein are in feet referred to the National Geodetic Vertical Datum (NGVD).

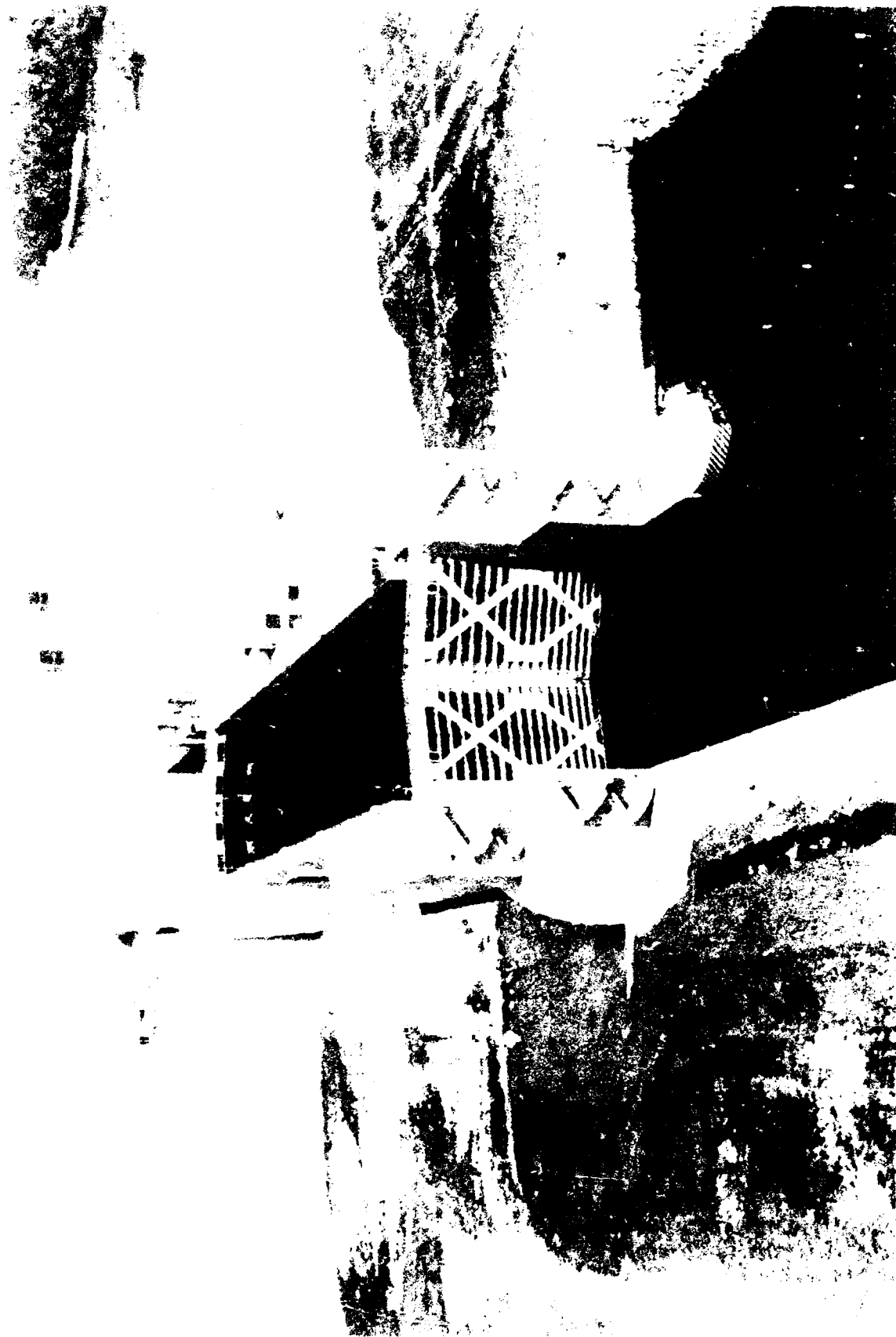


Figure 2. Bay Springs Lock and Dam

half of the lock chamber in conjunction with two tuning forks leading to the four longitudinal floor culvert manifolds; and outlet laterals in which the left culvert discharge lateral is located to the left of the guard wall and the right culvert discharge lateral is positioned between the lock approach walls. The flow is distributed into the chamber through a total of ninety-six 3.5- by 1.5-ft ports.

### Purpose and Scope of the Study

#### Purpose

4. The primary purposes of the prototype tests were to (a) determine the operating characteristics and hydraulic efficiency of the lock, (b) evaluate the accuracy of both physical and analytical model test predictions, and (c) evaluate important design factors such as the cavitation parameter and the effects of venting and submergence. Determinations of prototype discharge and loss coefficients for the culverts and valves were secondary objectives. Measurements were also made to determine the surges in the downstream canal from Bay Springs to Lock and Dam E generated by emptying.

#### Scope

5. Twenty-four tests, each performed under different conditions, were conducted at Bay Springs Lock during 1-3 August 1985. The types of tests conducted were (a) normal filling and emptying, (b) filling valve operations to determine incipient cavitation/airflow and effects of submergence, (c) different air vent configurations (orifice, full open, and closed vents), and (d) the steady-state flow condition. Individual tests of these types varied with respect to the valve times, single or dual valve operation, and for the steady-state condition, different filling valve openings.

### Prior Model Studies

6. Previous model studies of the lock have been conducted by the US Army Engineer Waterways Experiment (WES), including a 1:25-scale model reproducing 700 ft of the upstream approach, the entire filling and emptying system, and approximately 600 ft of the downstream approach (Ables 1978); and a 1:80-scale model of the diffuser system and lower approach area from the downstream miter gates of the lock to a point 3,500 ft downstream in the canal (Tate 1978).

## PART II: MEASUREMENTS, EQUIPMENT, AND PROCEDURES

### Measurements and Equipment

7. Locations of the test instrumentation are shown in Plates 1 and 2. The specifics of each transducer are listed in Table 1. The following paragraphs describe the transducers according to type of measurement.

#### Air vent flow rate (AVL, AVR)

8. Dual 12-in.-diam air ducts lead to each side of the culvert roof immediately downstream of the filling and emptying valves as shown in Plate 2. The airflow at the filling valves is controlled by 6-in.-diam orifices at the two duct intakes for each valve. The orifices were sized during a field reconnaissance trip to Bay Springs Lock in December 1984.\* The orifice size was optimized to provide adequate airflow to relieve the low pressures below the valve without causing excessive chamber turbulence. The airflow for this vented condition was measured for the left-wall filling valve with transducers AVL and AVR, located 4.5 in. radially outward from the center of each orifice plate as shown in Figure 3. Specifically, the transducers measured the absolute pressure at the back side of the plate near the vena contracta of the inflowing jet. This measured pressure drop across the orifice plate was proportional to the air velocity through the orifice. The emptying valve duct intakes remained fully open and were not monitored.

#### Downstream canal surge (DS1, DS2, DS3)

9. Water-level measurements were made at three locations in the downstream canal from Bay Springs to Lock E for the purpose of determining the surges generated by lock emptying. A 15-psia pressure transducer, DS1, located in a ladder well along the left guide wall directly above the right culvert discharge lateral, was the uppermost gage. This gage was incorporated into the WES recording system and continually monitored during emptying tests. DS2 was located at the Mackey's Creek Minimum Flow Structure 1.69 miles downstream. DS3 was located 5.15 miles downstream of Bay Springs at Lock E. Both DS2 and DS3 were Leupold-Stevens Model A-71 water level recording gages with quartz multispeed timers. These gages and the personnel to operate them were

---

\* F. M. Nielson. 1984 (Nov). "Trip Report, Bay Springs Lock, 14-15 November 1984," Memorandum For Record, US Army Engineer Waterways Experiment Station, Vicksburg, MS.



Figure 3. Air vent flow rate instrumentation

provided by the US Army Engineer District, Mobile. The specifics of the surge instrumentation are given in Table 1.

Miter gate opening (GDL, GDR, GUL, GUR, MSU, MSD)

10. Movement of the miter gates caused by overfilling (upstream gates) or overemptying (downstream gates) was monitored to obtain the time initial gate opening occurred and the total arc of opening. Microswitches were mounted on the mating edges of each pair of upstream (MSU) and downstream (MSD) miter gates to record the time of initial gate opening. Angular potentiometers (GDL, GDR, GUL, GUR) were mounted at the point of rotation of each miter gate such that any movement of the gates was continually monitored during each test. An aluminum rod extended from the axis of the potentiometer to a fixed point on the lock to rotate the potentiometer shaft.

Culvert roof pressures (LC1, P5)

11 Facilities for five flush-mounted pressure transducers were installed in the center line of the left culvert roof during construction of Bay Springs Lock at the locations shown in Plate 1. These consisted of an embedded transducer mounting box and cable passage with a pull wire extending to an easily accessible location such as the service gallery or valve cylinder recess. Two interchangeable cover plates were fabricated for each mounting

box, one for permanent cover and one, as shown in Figure 4, to be used by WES to install the pressure transducer just prior to testing. Because the lock could not be dewatered, all culvert transducers were installed by divers.

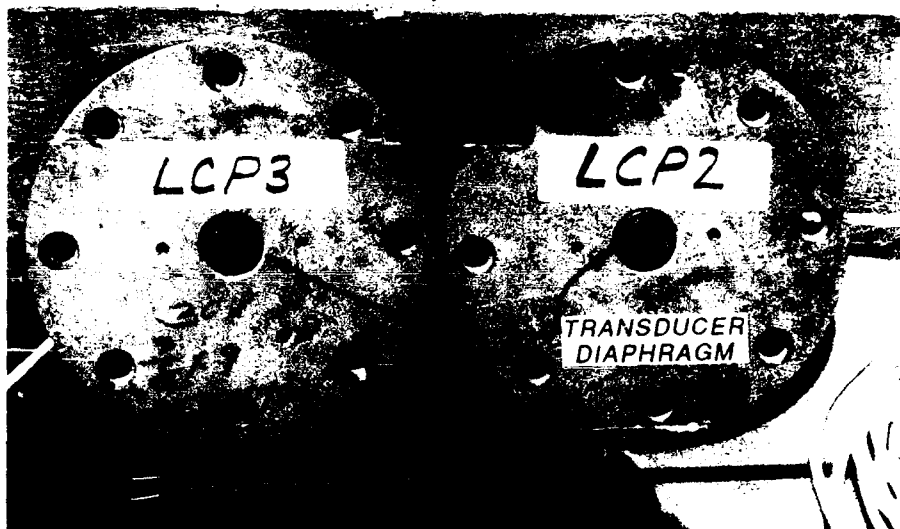


Figure 4. Culvert transducer mounting plates

12. Transducers LCP1 and LCP5 measured the average and fluctuating pressures in the highly turbulent flow immediately downstream of the left wall filling and emptying valves, respectively. Information from transducers LCP2, LCP3, and LCP4 was to be used for measuring the energy grade line of the culvert to determine head losses. However, only transducer LCP2 could be installed. Locations LCP3 and LCP4 were not instrumented because the transducer mounting box cover plates could not be removed and replaced with the transducer plates.

#### Lock water-surface elevation (LWSE)

13. The lock water-surface elevation was measured continually for each test with a 100-psia pressure transducer, LWSE, located at el 326.1 in the lock chamber. The transducer, as shown in Figure 5, was mounted in a pipe adapter and rigidly attached to ladder rungs in the center left-wall ladder well (monolith L24).

#### Valve opening (VEL, VER, VFL, VFR)

14. Movement of any operating tainter valve (filling or emptying) was monitored for the duration of each test. The measuring devices were angular potentiometers attached to the remote indicator unit such that any valve movement (opening or closing) caused a rotation of the potentiometer (Figure 6).

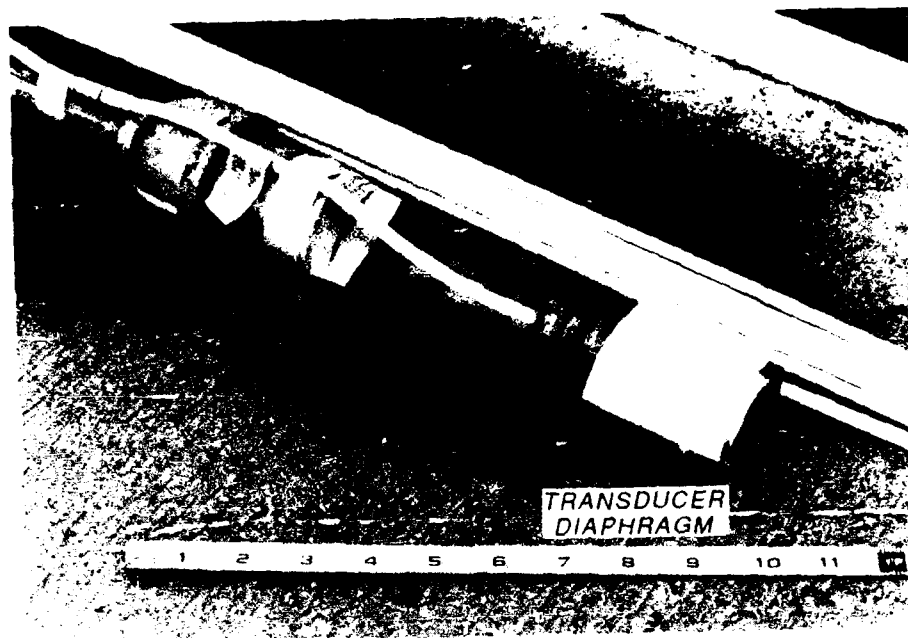


Figure 5. Lock water-surface elevation transducer

Valve cylinder pressure (VHP1, VHP2)

15. Pressures in the hydraulic cylinder of the left-wall filling valve were continuously monitored for the duration of each filling test. One 2,000-psia pressure transducer (VHP1) measured hydraulic pressure on the lowering side of the piston; a 2,500-psia pressure transducer (VHP2) measured the pressure on the raising side of the piston. These locations are shown in Plate 2.

Valve well water-surface elevations (WSEL, WSER, WSFL, WSFR)

16. Filling and emptying valve well water-surface elevations, or valve well piezometric head, were measured by pressure transducers for all valve wells. These transducers, housed in watertight adapters and mounted to pipes identical to that shown in Figure 5, were secured to grease lines on each valve well wall (upstream side) at elevations below minimum water levels. The location and description of each transducer are given in Plates 1 and 2 and Table 1.



Figure 6. Tainter valve movement indicator

### Water-surface drawdown at intakes (WSI)

17. A 15-psia pressure transducer (WSI) was used to monitor the water-surface elevation of the upstream approach during filling operations. This transducer was rigidly attached to ladder rungs, below the minimum water level, in the ladder well in monolith 14 on the left approach wall (Plate 1). The primary purpose of this measurement was to determine the amount of water-surface drawdown in the approach in the vicinity of the intakes.

### Recording Equipment

18. The transducer cable lengths required for the test program were determined from contract drawings and actual measurements at the project. These cable lengths (listed in Table 1) were cut and used in the calibration of their corresponding transducers to account for line losses. A total of 4.2 miles of cable was required for the Bay Springs test program.

19. The recording equipment consisted of (a) WES-fabricated model 03 bridge amplifiers to condition transducer signals, (b) WES-fabricated recording interface panel for simultaneous amplifier calibration steps, tape recorder event mark, and tape recorder voice-record and -reproduce capabilities, (c) Datum model 9300 time code generator for recording IRIG-B time code, (d) H/P model 3490A multimeter, (e) H/P model 5532A electronic counter, (f) WES-fabricated 12-channel playback attenuation panel, (g) a Sangamo model Sabre V, 32-track magnetic tape recorder with a frequency response of DC to 40 kHz, (h) a 36-channel CEC model 5-119, 12-in. chart, direct-record oscillograph, capable of reproducing data at various chart speeds from 0.125 to 160 ips at a frequency response dependent upon the type galvanometer being used, (i) CEC model 7-364 galvanometers with a frequency response of DC to 500 Hz, and (j) a Ballantine model 1022A dual-channel oscilloscope that was used in conjunction with the H/P multimeter and H/P counter for system calibration and periodic data checks during testing. Figure 7 shows equipment setup at the recording station.

### Testing Procedure and Conditions

#### Types of tests

20. During all tests there were no tows or vessels in the lock chamber.

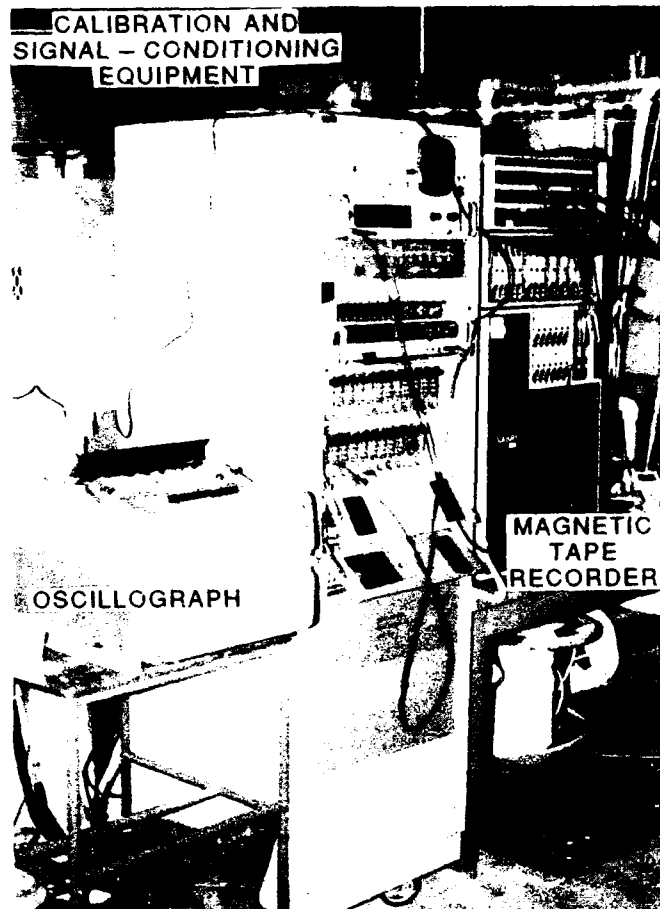


Figure 7. Recording station and equipment

The testing program is grouped into five series as follows:

- a. Filling and emptying tests (FE series). This series, consisting of 10 runs, was primarily concerned with the overall performance of the lock during filling and emptying operations. During these tests the chamber was being either filled or emptied and the data recorded continuously during the entire locking operation. Two general types of filling and emptying tests were conducted: (1) allow the chamber pool to overflow or overempty to the maximum, and (2) minimize the overtravel (normal operations). To allow maximum overtravel, the valves were held fully open throughout the entire operation. Normally, to minimize overtravel, when the chamber-to-pool differential elevation reached 2 ft, the valves were lowered to approximately 2 ft open and held for 1 to 5 sec, then returned to fully open.
- b. Incipient airflow and cavitation tests (CA series). This series of tests was concerned primarily with determining the design parameters of incipient cavitation and airflow below the filling valves. The test procedure followed was different from

the regular filling procedure. An initial differential pressure was set on the filling valves by setting the lock chamber water surface to an elevation higher than the predicted incipient differential. Once the desired elevation was set, the filling valve(s) were opened at the appropriate rate; and the severity of the cavitation, if any, and the quantity of airflow were determined. A new chamber elevation was then set and the procedure repeated until the chamber elevations at which cavitation and airflow just began were determined.

- c. Steady-state tests (SS series). This series of four tests was conducted to determine various prototype coefficients such as discharge and contraction coefficients for the valves, for comparison with those used in the analytical model. These can be most accurately determined by establishing a steady-state flow condition through the lock culvert system. This condition was established by first setting the chamber to full pool elevation and then setting the left-wall filling valve to a specific opening. Next, the opposite (right wall) emptying valve was fully opened, allowing the system to equalize the inflow and outflow. This steady-state condition was maintained for 1-2 min before the emptying valve was closed to fill the lock.
- d. Air venting tests (AV series). This series was designed to evaluate pressures below the filling valves and lock chamber water-surface turbulence resulting from different air vent configurations. The filling valves at Bay Springs are normally vented with a 6-in. orifice plate installed at the vent intakes. For these tests, the vents were either fully opened to their maximum 12-in. diam (orifice plates removed) or were completely closed. The vents for the emptying valves remained fully open during all tests.
- e. Valve tests (VP series). These tests involved raising and lowering the left-wall filling valve under upper static conditions; that is, the chamber water surface was maintained at upper pool elevation. The pressures in the hydraulic cylinder were measured.

#### Test variables

21. The variable specifics for each test are listed in Table 2. For the FE and VP series, the valves were the lock components that were controlled. Two nominal valve times were used for filling tests: fast (1 min) and slow (4 min). For emptying, nominal valve times used were 2 and 4 min. In addition, both synchronous and single-valve operations were performed.

22. For the CA series, the components controlled were the valve rate and the initial chamber elevation. Test sequences for fast and slow valve times were conducted. In each sequence, the initial chamber elevation was varied for individual runs to determine the desired incipient values.

23. The lock component controlled during the SS series was the valve opening of the left-wall filling valve.

Test conditions

24. Pretest and posttest upper, chamber, and lower pool elevations were observed visually from the upper, chamber, and lower pool staff gages. These data and brief descriptions of the conditions during each run are listed in Table 2.

Recording Procedures

25. Individual tests were recorded on magnetic tape for the duration of time as indicated in the following tabulation:

<u>Type of Test</u>	<u>Duration of Data Record</u>
FE	Complete fill or empty operation
CA	Valve operation
SS	Steady-state condition till lock filled
AV	Valve operation
VP	Valve operation

A portion of the taped data was transferred to oscillograms to confirm that the data were being recorded properly.

26. The recording procedure was generally the same for all tests and consisted of the following:

- a. Set and read such initial test conditions as pool elevations and valve opening.
- b. Record pretest zero levels.
- c. Record transducer step calibrations.
- d. Record initial static conditions.
- e. Record test data (refer to types of tests, paragraph 20).
- f. Record final static conditions.
- g. Record posttest transducer calibrations.
- h. Record posttest zero levels.
- i. Prepare for next test.

27. Voice comments on the tape and notes on the oscillograms were continuously made for later reference. Calibration changes were made as required during the test period.

### Analysis Procedures

28. The data reduction and analysis were performed by personnel of the Hydraulic Analysis Branch (HAB) at WES. All data channels were recorded and reduced simultaneously providing a direct time-dependent relationship among all channels. The data reduction included digitizing the data, fine-tuning the pretest transducer calibrations, and performing all appropriate analyses needed to present the results in the desired form. These were all performed using HAB's Data Acquisition and Reduction System (DARS).

## PART III: BASIC LOCK PERFORMANCE

### Lock Performance Parameters

29. General lock performance was evaluated by a sequence of varying filling and emptying procedures. These are referred to as type FE tests and are described in detail in paragraph 20a. Figure 8 is a definition sketch showing the important parameters measured for evaluating lock performance.

30. During filling and emptying runs, the valve movement is initiated at time\*  $t = 0$  and reaches fully open at time  $t = t_v$ . The initial differential head  $H$  is the difference between the upper and lower pools, i.e.,  $H = Z_U - Z_L$ . The rate of rise of the water surface  $dz/dt$  increases from time zero to a maximum at time  $t_m$ , after which it decreases continually, reaching zero at time  $t_f$ . The operation time, or filling (emptying) time, is designated as  $T$ . The inertia of the water in the filling system causes the water surface to rise above the upper pool after time  $T$ . This overtravel (or overfill) is defined as the distance  $d_f$  and occurs at time  $t_f$ . During emptying, the overtravel (or overempty) extends below the lower pool the distance  $d_e$  at time  $t_e$ .

### Valve Operation

31. Valve movement was measured by transducers VFL, VFR, VEL, and VER as described in paragraph 14. Any movement by the valve produced an angular rotation measurement in degrees. This relative motion measurement was converted to actual valve position, i.e., the height in feet above the invert of the culvert, by a relationship based on the geometry of the valve and valve linkage. Also taken into consideration was the slack in the linkage due to the spring assembly located at the top of the upper strut. Figure 9 presents this valve opening calibration in terms of percent valve opening  $b/B$  versus percent of valve time. Also shown is the predicted valve opening schedule presented in the design drawings and the valve sag value used in the Corps' analytical model of lock operation from the Conversationally-Oriented

---

\* For convenience, symbols and unusual abbreviations are listed and defined in the Notation (Appendix A).

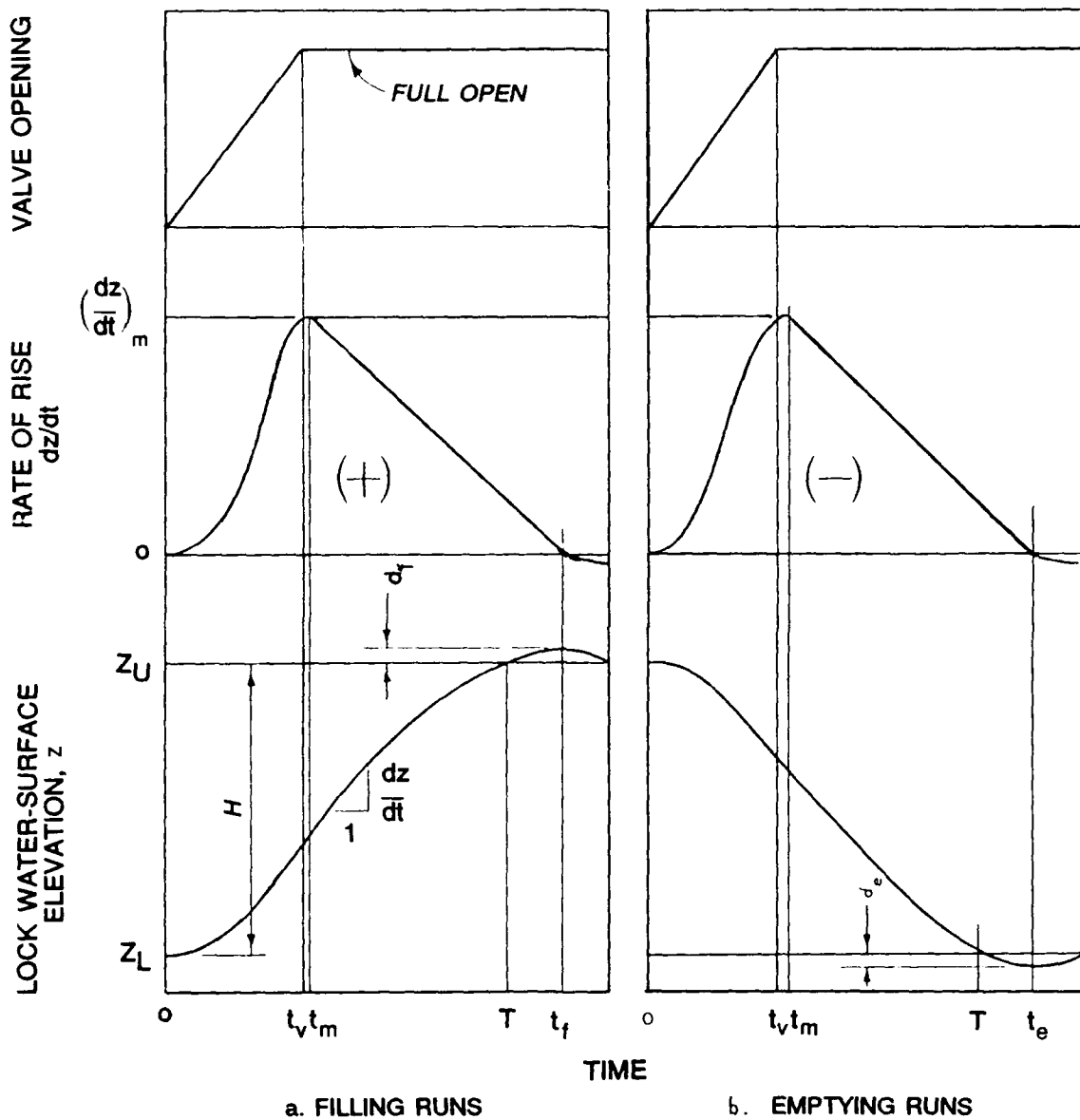


Figure 8. Definition sketches of the filling and emptying runs

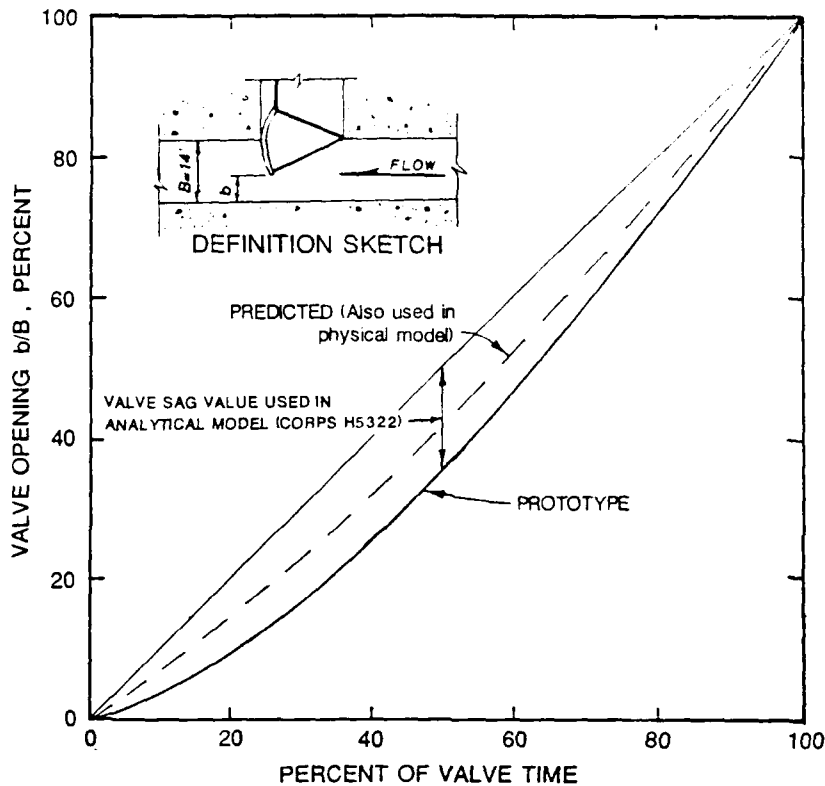


Figure 9. Valve opening calibration

Real-Time Programming System (CORPS), H5322 (Neilson and Hebler 1988). All valves were assumed to be identical. A diagram of the valves is shown in Plate 2.

32. Table 2 presents the nominal valve rates tested. For filling, the nominal rates were 1 and 4 min, and for emptying, 2 and 4 min. The faster rates are the normal operating condition. Actual valve operation times for each FE test are given in Table 3. Plates 3-5 show the measured valve patterns for all filling and emptying operations. For the two-valve operations, the valves acted in synchronization, except for a few seconds' delay of the right-wall valves on some tests, which is considered insignificant.

#### Valve Hoist Loads

33. Valve cylinder pressures were monitored on the left-wall filling valve for no-flow (submerged) and normal operating conditions. The differential pressure between the raising and lowering side of the piston was measured and then translated into tangential force at the valve pickup (kips). This

force was computed by converting the measured net force on the piston rod to tangential force using the force diagrams given in the design drawings. Plate 6 presents the measured differential valve cylinder pressures and tangential forces along with the predicted. Under no-flow conditions, the pressures, as well as the forces, required to open the valve were practically equal for both the 1-min and the 4-min nominal valve rates. The force required to raise the submerged weight of the valve ranged from 30 to 40 kips. With flow, the maximum force occurred at the 1-ft valve opening, reaching 146 and 125 kips for 1-min (Test FE7) and 4-min (Test FE5) nominal valve rates, respectively. These are approximately double the predicted required forces. However, they are still considerably less than the available force, which is based on 850-psi differential cylinder pressure. The maximum differential cylinder pressure occurred at the 2-ft valve position and reached 800 psi for Test FE7 and 700 psi for Test FE5.

34. The hydraulic loads on the tainter valves (hoist loads) are equal to the summation of the forces on the valve members due to flowing water and are considered in terms of uplift and downpull loads. Downpull loads act to rotate the valve to the closed position and uplift loads act to rotate the valve to the open position. The uplift and downpull loads are equal to the vertical (y) component of the tangential force at the valve pickup during normal operations less the vertical component of that portion of the force required to raise the submerged weight of the valve. Figure 10 presents the measured hoist loads. At no time were any uplift forces observed for the left-wall filling valve. A high downpull load of 103 kips occurred at the 1-ft opening for the 1-min valve rate. Loads for the 4-min valve rate (FE5) were approximately 30 percent lower. The load then decreased to approximately 19 kips when the valve was nearly fully open. These results differ from the predicted loads (refer to Figure 10) suggested by Engineering Manual (EM) 1110-2-1610 (Headquarters, US Army Corps of Engineers (USACE), 1975). The hoist load curves given in the EM are the result of model tests conducted under steady-state conditions. Each of the following conditions may affect the predicted versus prototype correlation: drawdown in the valve well, pressures just downstream of the valve, possible different flow patterns in the prototype, and differences in construction of the prototype.

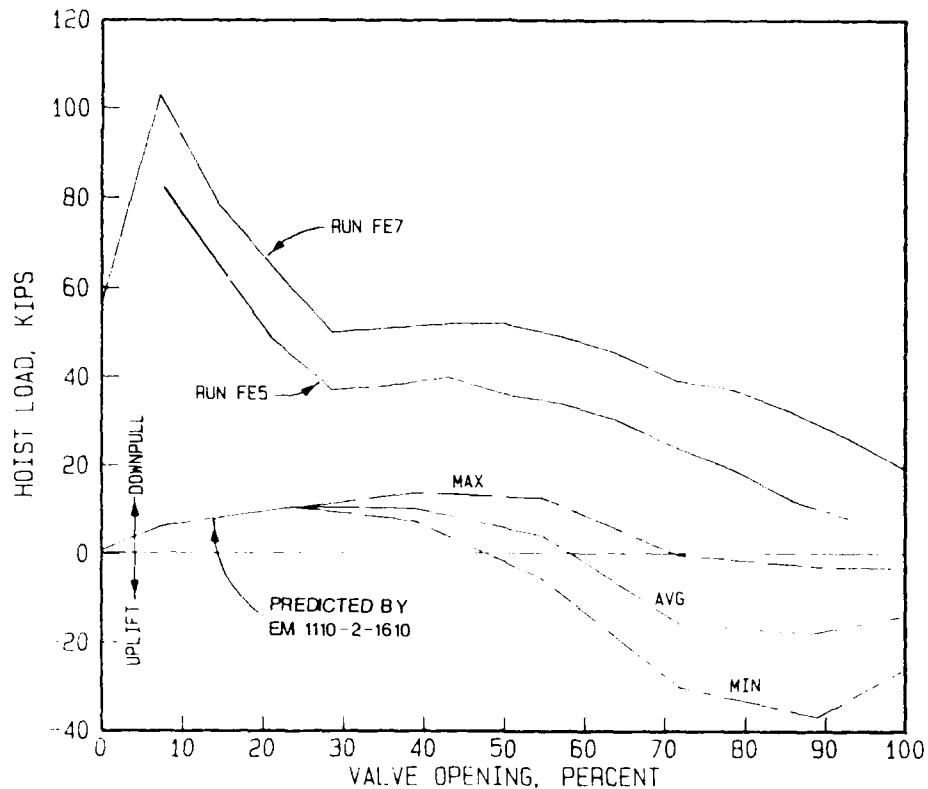


Figure 10. Hydraulic loads on tainter valve

### Filling and Emptying

#### Operation times

35. Operation times for filling and emptying the lock are listed in Table 3. The filling and emptying curves are shown in Plates 7-10. The lock water surface for Tests FE1 through FE8 was allowed to overtravel for the purpose of determining the full operation times required by the filling and emptying system. Tests FE9 and FE10 were conducted using normal operation procedures to determine the actual operation time at Bay Springs. As shown by Plate 5, the valves for emptying, Test FE10, were closed just prior to the water surface reaching full pool to approximately 20 percent open, held for a few seconds, and returned to fully open. This is the correct procedure and was used for the purpose of minimizing the amount of overtravel. As expected, the operation time was longer for the normal empty test (FE10) than for the test with overtravel (FE2). These measured times were 798 and 704 sec, respectively. Also contributing to this longer operation time was the 0.9-ft difference in initial head as well as the changing lower pool elevation during

emptying. Table 4 lists the initial and final empty pool elevations. For the filling test FE9, the valves were not closed until the lock was filled, were allowed to close completely, and were then never reopened. This is not considered the normal operating procedure and did not affect the operation time (refer to Tests FE3 and FE9 in Table 3).

#### Overtravel

36. As stated in paragraph 35, Tests FE1 through FE8 were performed to permit overtravel. This required maintaining the valves fully open during the entire operation and keeping the appropriate miter gates closed for as long a time as they could safely withstand any reverse head caused by the overtravel. Except for Tests FE5 and FE6, the miter gates had to be slightly opened prior to the time the chamber water surface reached maximum overtravel to prevent their possible failure. Therefore, the measured overtravel may be somewhat less than what would be expected had the gates been held closed throughout the entire operation. Table 3 lists the amount of overtravel ( $d_f$  or  $d_e$ ) and the time when it occurred for each FE run. It should be noted that for Test FE10, which was performed to minimize the overtravel, none was measured.

#### Air demand

37. The admission of air into the culverts just downstream of all valves at Bay Springs was required to eliminate the damaging cavitation that would occur without adequate venting. Significant airflow existed for all filling and emptying operations such that the amount of venting needed to be controlled, or optimized, to prevent excessive amounts of air from reaching the chamber water surface and causing potentially dangerous surface turbulence. As described in paragraph 8, a 6-in.-diam orifice was used on the air intakes of the filling valves to control air entrainment. The emptying valves were not provided any air throttling. Tests were conducted to evaluate qualitatively the effects of excessive airflow on chamber surface conditions as a concern to navigation. With the orifices installed, chamber conditions were excellent with only mild to moderate surface turbulence noted. Small craft felt virtually no effects. Tests AV-1 and AV-2 were conducted with the vents fully open (orifice plates removed) for a single valve at both the 1- and 4-min rates. Although no airflow measurements were made, field observations noted an increase in airflow for the 1-min valve rate and only slightly more turbulent chamber conditions. Airflow for the 4-min valving was noted to be considerably higher. Airflow was very intense at the air intakes and the

surface conditions were considered moderately severe. Although no hawser measurements were made, it was concluded through these visual observations that the turbulence caused by air entering the chamber for the 4-min valve fully open vent condition was excessive and potentially hazardous to vessels, especially small craft, during lockage.

38. The airflow rate  $Q_a$  is given by

$$Q_a = \pm C_d A \sqrt{\frac{2|\Delta P|}{\rho_a}} \quad (1)$$

where

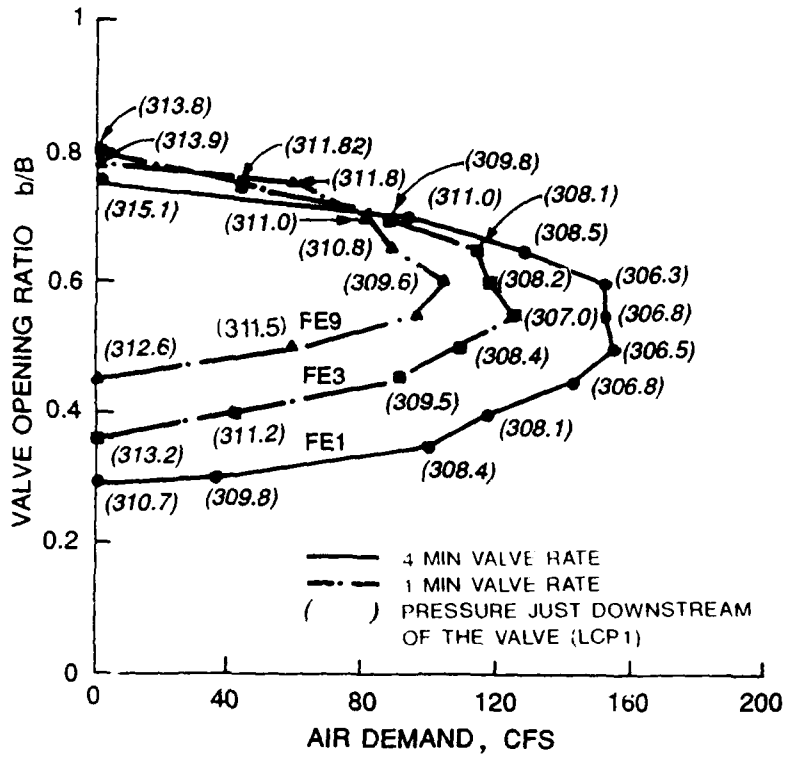
$C_d$  = orifice discharge coefficient

$A$  = orifice area, in.<sup>2</sup>

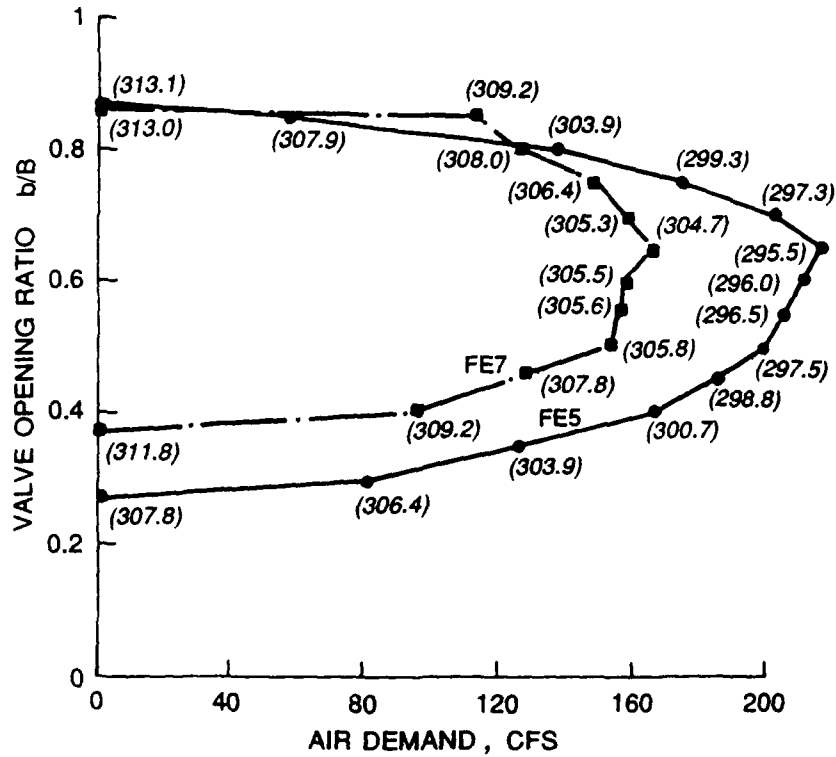
$\Delta P$  = difference in pressure head immediately upstream and downstream of the orifice (refer to Figure 3), psid

$\rho_a$  = mass density of the air, lb/in.<sup>3</sup>

A value for  $C_d$  of 0.60 (Howe 1950) was used for all calculations. The absolute value of the differential  $\Delta P$  was obtained from pressure transducers AVL and AVR (see paragraph 8 and Figure 3). Measurements were made only for the left-wall filling valve. Plate 11 shows a typical airflow time-history with culvert pressure and valve motion. A negative  $\Delta P$  indicates air flowing into the duct, and a positive  $\Delta P$  indicates air flowing out of the duct. The higher frequency pressure fluctuations present on AVL and AVR signals are acoustical and not representative of actual airflow and were therefore filtered during analysis to render the most accurate measures of airflow. The airflow rates for the left-wall filling valve are shown in Figure 11. Air was drawn into the culverts between  $b/B$  values of approximately 0.30 and 0.80 (see Figure 11). As expected, airflow rates are considerably higher for the 4-min valve versus the 1-min valve just as the airflow rates are higher for single-valve versus synchronous-valve operation. This shows the sensitivity of the airflow to small differences in pressure at the culvert roof  $\left(\frac{p}{\gamma_w}\right)_r$ . Values of  $\left(\frac{p}{\gamma_w}\right)_r$  varied for these different test conditions as the water-surface rate of rise varied. In other words, the higher the chamber elevation, or submergence, the higher the culvert pressure. The mean piezometric head elevations measured by transducer LCPI are also included in Figure 11. The pressures at LCPI were below the roof of the culvert (el 312.0) during



a. Synchronous valve filling



b. Single valve filling

Figure 11. Airflow rates for left-wall filling valve

airflow. However, no damaging cavitation conditions existed due to sufficient cushioning of the negative pressures by the air supplied by the vents. A detailed discussion of the correlation of airflow and culvert pressures will be addressed later in this report.

39. Kalinski and Robertson (1943) found the ratio of the air demand to water discharge ( $Q_a/Q_w$ ) to be a function of the Froude number minus one in a conduit operating under hydraulic jump conditions. These conditions exist in the filling and emptying systems of navigation locks in the conduit just downstream of the valves during valve opening. USACE combined this information with field measurements and derived a suggested design curve. The Bay Springs Lock air vent discharges shown in Figure 11 were plotted on the Hydraulic Design Criteria (HDC) chart (USACE) reproduced in Plate 12. The Froude number  $IF$  for the data was computed by

$$IF = \frac{V}{\sqrt{gy}} \quad (2)$$

where

$V$  = water velocity at the vena contracta, fps

$g$  = gravitational acceleration, ft/sec<sup>2</sup>

$y$  = water depth at the vena contracta, ft

The air demand is controlled by the capacity of the hydraulic jump to entrain and remove air. At Bay Springs, the airflow is further controlled by the throttling effects of the orifice plates (all data presented in Plate 12 were measured with 6-in. orifice) and the pressures below the valve. Also, as stated earlier, a considerable increase in the airflow was observed for the fully open vents. These factors indicate that the total air demand for the hydraulic conditions was not reached even though the actual quantity was more than sufficient to prevent extreme cavitation.

#### Water-surface drawdown at intakes

40. Water-surface elevations in the vicinity of the intakes were monitored during all tests by pressure transducer WSI at monolith L15 (see Plate 1). The placement of the gage was not directly above the intakes, but approximately 20 ft downstream of the most downstream portal. Therefore, some difference between the actual maximum drawdown and that measured may exist. However, because of the relatively small surface area at the intake approach,

any difference should be quite small. Drawdown of the water surface occurred for all conditions tested, ranged from 0.11 to 1.08 ft, and occurred as the valve(s) approached fully open. The amounts for individual tests are given in the following tabulation:

Test No.	Nominal Valve Time, min	No. of Valves	b/B	Drawdown ft
FE1	4	2	0.71	0.50
FE3	1	2	0.94	0.11
FE5	4	1	0.75	0.39
FE7	1	1	0.93	0.61
FE9	1	2	0.94	1.08

41. A vortex developed in the approach at Bay Springs during every filling operation. This vortex, as shown in Figure 12, was in the vicinity of the intakes at monolith 12. The size of the vortex was approximately 4-5 ft across and 2-3 ft deep. During normal operations, it would begin to form at about 4 min after the valves began, lasting 4 min before dissipating. It is not known from these observations whether or not the vortex tail reached the intakes. The vortex was not detected in model tests (Ables 1978). This can be attributed to the relatively small approach area and topography reproduced in the model.



Figure 12. Vortex formed in approach

### Downstream surge

42. The downstream canal has a base width of 300 ft and a depth of 13 ft at normal water surface (el 330), which is controlled by Lock and Dam E located 5.2 miles downstream. Bay Springs Lock, in a relatively short period of time, empties approximately 6.2 million cubic feet of water into the canal during each lockage, creating an appreciable surge in the canal. This large quantity of water introduced to the confined canal also causes fluctuations in the water-surface elevation of the canal through storage that requires regulation by releases at Lock and Dam E. Table 2 lists the canal pool elevations at the start of each test. Elevations ranged from as low as 329.3 to a high of 330.9. Also contributing to this fluctuation in canal water-surface elevation was the reflection of the surge as it encountered the pool at Lock E.

43. It was concluded in the physical model study (Tate 1978) that the slope of the water surface rather than the surge height is the critical factor affecting the forces exerted on tows in the canal. Measurements of the surge were made as described in paragraph 9 for all empty runs, and the time-histories are presented in Plate 13. The data summary of Table 5 includes measures of the surge height and the maximum water-surface rate of rise. These values vary with the number of valves and the valve rates used in emptying the lock. At gage location DS1, the maximum surge height (4 ft) and the maximum rate of rise (0.07 fps) occurred at the two-valve, 2-min nominal valve rate (FE10). Accordingly, the minimums occurred at the one-valve, 4-min valve rate (FE6). Approximately 2 miles downstream at the Mackey's Creek flow control structure, the surge height was reduced by one-half.

44. The prototype and physical model results were compared for the prototype run FE10. For this 2-min, synchronous emptying valve schedule, the model predicted a maximum rate of rise of the water surface at the prototype DS1 location to be 0.06 fps with a maximum surge height 2.5 ft above normal pool. The prototype values were 0.07 fps and 4.0 ft, respectively. Figure 13 presents the measured water-surface elevations of the surge for both the model and prototype.

45. Another tool available for predicting surges is the Corps' analytical model for surges in navigation channels, the CORPS program, H5310 (Neilson 1979). Output from H5310 runs at the tested prototype conditions are as follows:

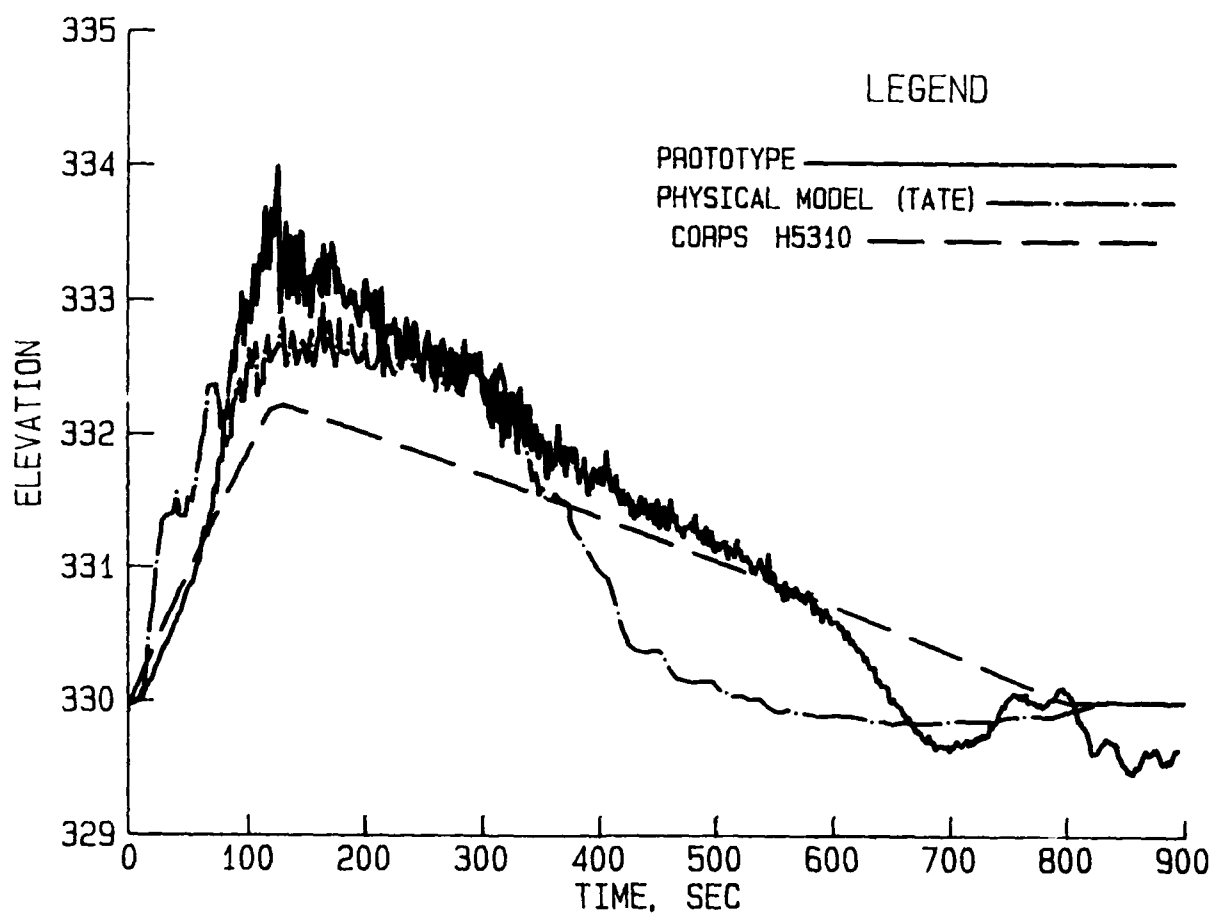


Figure 13. Model-prototype comparison of downstream canal surge, 2-min synchronous valving

Test No.	Condition		Location	Surge Height, ft		Time to Max, sec*		Wave Celerity, fps**	
	No. of Valves	Nominal Rate min		Proto-type	H5310	Proto-type	H5310	Proto-type	H5310
FE2	2	2	DS1	3.4	2.4	128	120		
			DS2	2.4	2.4	456	441	25	25
FE4	2	4	DS1	3.2	2.2	190	200		
			DS2	1.6	2.2	420	517	35	25
FE6	1	4	DS1	1.2	1.3	239	210		
			DS2	1.0	1.3	495	550	32	24
FE8	1	2	DS1	1.3	1.2	129	120		
			DS2	1.0	1.2	552	459	19	24
FE10	2	2	DS1	4.0	2.2	126	130		
			DS2	2.1	2.2	459	448	24	25

\* Time after valves begin that crest of surge reaches location.

\*\* Celerity measured between locations DS1 and DS2.

Not considered in H5310 are effects of channel friction, surge reflections, and water storage/releases (Lock E), which are all factors affecting the prototype. This accounts for the constant surge height given in the tabulation for H5310 runs as the surge progressed downstream. Wave celerity as computed between locations DS1 and DS2 compared well between the model and prototype. The surge calculated by H5310 for run FE10 is shown in Figure 13.

Culvert discharge coefficient

46. The discharge coefficient  $C$  of the hydraulic system is based on the equality of the rate of rise of the lock chamber water surface and the rate of flow through the culvert(s). It is determined as

Filling:

$$C = \frac{A_L \frac{dz}{dt}}{A'_C \sqrt{2g(Z_U - z)}} \quad (3)$$

Emptying:

$$C = \frac{-A_L \frac{dz}{dt}}{A'_C \sqrt{2g(z - Z_L)}} \quad (4)$$

where

$A_L$  = water-surface area of the lock chamber

$A'_C$  = representative cross-sectional area of the culvert(s)

$z$  = elevation of water surface in the lock chamber

47. The coefficients were determined for the time period beginning at  $t_v$  to the time the elevation of the water surface in the lock chamber reached the elevation of the upper miter gate sill (el 390). This endpoint was used because the water-surface area of the lock chamber differed above and below this elevation by the cross-sectional area of the miter sill inside the lock chamber (refer to Plate 1). Therefore, for filling runs, the value for  $A_L$  used was 72,380 sq ft and represented the area below el 390. For emptying,  $A_L$  was 73,700 sq ft and represented the area above el 390. These values for  $A_L$  were scaled from the construction drawings and are used throughout this

report. The coefficients calculated using Equation 3 are listed as follows:

Filling			Emptying		
Test No.	Valve Operation	C	Test No.	Valve Operation	C
FE1	Synchronous	0.743	FE2	Synchronous	0.629
FE3	Synchronous	0.741	FE4	Synchronous	0.624
FE5	Single	0.794	FE6	Single	0.683
FE7	Single	0.794	FE8	Single	0.667
FE9	Synchronous	0.747	FE10	Synchronous	0.624

Average values of  $C$  for the synchronous and single-valve filling runs are 0.744 and 0.794, respectively. The emptying values are 0.626 and 0.675, respectively, for the synchronous and single-valve operations.

#### Lock design equation

48. A relationship between operation time, lock chamber area, and total lift is required for lock design. This relationship is expressed by the traditional empirical lock design equation (Headquarters, USACE, 1956) or Pillsbury's equation

$$T - kt_v = \frac{2A_L}{\sqrt{2g} C_L A'_c} (\sqrt{H + d_o} - \sqrt{d_o}) \quad (5)$$

where

$k$  = overall valve coefficient

$C_L$  = overall lock coefficient (comparable to the discharge coefficient  $C$  of Equations 3 and 4)

$d_o$  = overtravel, ft

49. Equation 5 is based on a solution for lock filling in which inertial effects are accommodated by incorporating overtravel into the final solution. The equation applies to both filling and emptying runs, provided  $d_f$  or  $d_e$  is properly substituted for  $d_o$ . The lock design equation was used for the experimental determination of  $C_L$  and to compare model and prototype efficiencies. Using an average value, 72,710 sq ft, for  $A_L$  and a nominal design value of 0.5 for  $k$ , values of the overall lock coefficient are as follows:

Filling			Emptying		
Test No.	Valve Operation	C	Test No.	Valve Operation	C
FE1	Synchronous	0.721	FE2	Synchronous	0.585
FE3	Synchronous	0.722	FE4	Synchronous	0.566
FE5	Single	0.766	FE6	Single	0.642
FE7	Single	0.771	FE8	Single	0.638

Average values of  $C_L$  for the synchronous and single-valve filling runs are 0.722 and 0.769, respectively. Discharge coefficients (paragraph 47) are about 3 percent greater. The emptying values are 0.576 and 0.640, respectively, for the synchronous and single-valve operations. Discharge coefficients are about 9 and 5 percent greater, respectively.

#### Valve coefficient

50. Operation times are shown in Figure 14 for filling runs from the FE series of tests and the physical model filling and emptying runs, adjusted to prototype pools (refer to paragraph 57). Prototype emptying runs are not presented because of the unknown effects of the tailwater rising over the outlets. The valve coefficient  $k$  is as the slope of the curves in Figure 14. As shown, the nominal design value,  $k = 0.5$ , is an acceptable fit to the experimental data for both model and prototype observations.

#### Overall loss coefficient

51. Basically, the overall head loss  $H_L$  in the system is considered to be made up of five manageable components as described in Equations 6-10 and as shown in Figure 15.

<u>Component</u>	<u>Head Loss</u>	
Intake	$H_{L1} = \frac{k_1 V_c^2}{2g}$	(6)

Upstream conduit	$H_{L2} = \frac{k_2 V_c^2}{2g}$	(7)
------------------	---------------------------------	-----

Valve and valve well	$H_{LV} = \frac{k_v V_c^2}{2g}$	(8)
----------------------	---------------------------------	-----

Downstream conduit	$H_{L3} = \frac{k_3 V_c^2}{2g}$	(9)
--------------------	---------------------------------	-----

Outlet	$H_{L4} = \frac{k_4 V_c^2}{2g}$	(10)
--------	---------------------------------	------

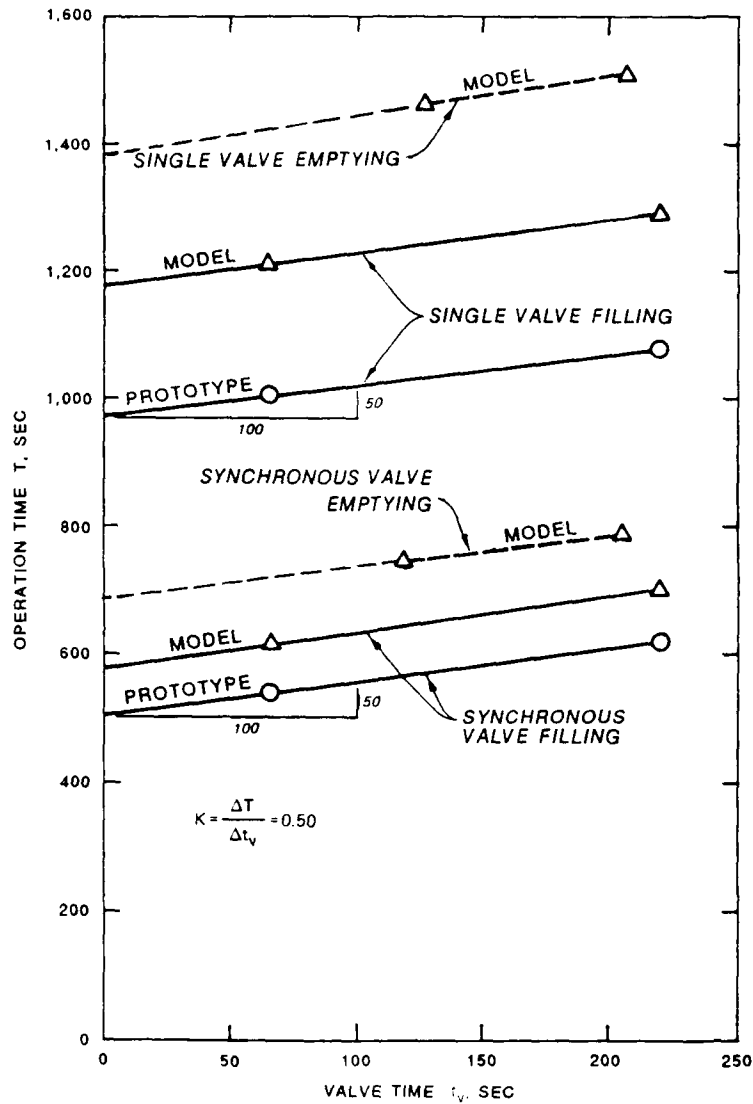


Figure 14. Lock operation time

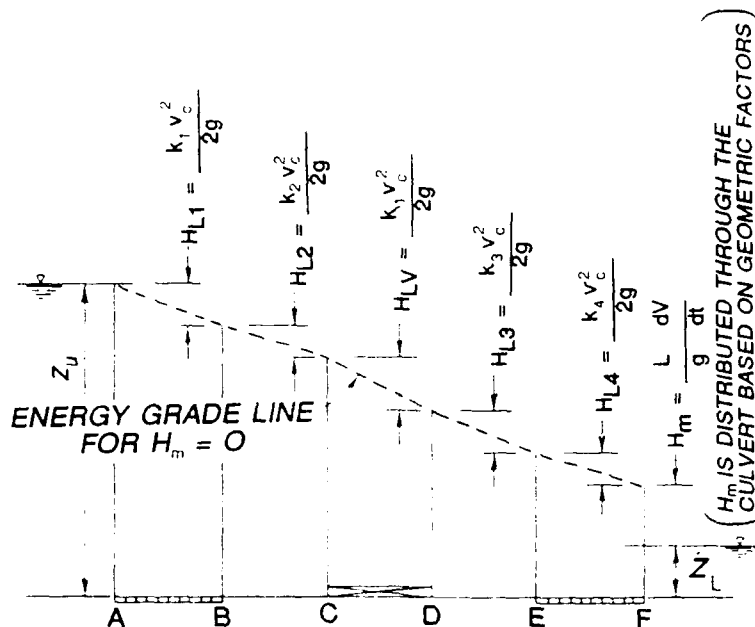
The overall loss,  $H_{Lt}$ , is

$$H_{Lt} = (k_1 + k_2 + k_v + k_3 + k_4) \frac{V_c^2}{2g} \quad (11)$$

or

$$H_{Lt} = \frac{k_t V_c^2}{2g} \quad (12)$$

where  $k_t$  is the overall loss coefficient and  $V_c$  is the average velocity of



SECTION	COMPONENT	FILLING		EMPTYING	
AB	INTAKE MANIFOLD	A IS IN UPPER POOL; B IS AT THE START OF THE CULVERT		A IS IN LOCK CHAMBER; B IS AT INTERSECTION OF CROSS-OVER AND CHAMBER MANIFOLD	
BC	UPSTREAM CONDUIT	C IS IN THE FILLING VALVE WELL		C IS IN THE EMPTYING VALVE WELL	
CD	VALVE AND VALVE WELL	D IS IMMEDIATELY DOWNSTREAM OF THE VALVE WELL		D IS IMMEDIATELY DOWNSTREAM OF THE VALVE WELL	
DE	DOWNSTREAM CONDUIT	E IS THE END OF THE CULVERT AND THE START OF THE CHAMBER MANI- FOLD		E IS THE END OF THE CULVERT AND THE START OF THE OUTLET MANIFOLD	
EF	OUTLET MANIFOLD	F IS IN THE LOCK CHAMBER		F IS THE LOWER POOL	

Figure 15. Definition sketch of system head loss

flow in the culvert. In practice, coefficients  $k_1$ ,  $k_v$ , and  $k_4$  are taken to be entirely form dependent (prototype evaluation of  $k_v$  is presented later in this report). Coefficients  $k_3$  and  $k_4$  are affected by both form and relative roughness. However, in view of the "stubby" conduits and the dominance of form effects in a lock system,  $k_3$  and  $k_4$  can reasonably be assumed constant for either model or prototype. All of the loss coefficients are affected by Reynold's number; therefore, significant differences will exist between the model and prototype values.

52. A brief description of the equations used to describe the unsteady lock flow is as follows. The flow is assumed incompressible and the inertial

effect is treated as a lumped quantity; that is,

$$H_m = \frac{L_m}{g} \frac{dV}{dt} \quad (13)$$

where

$H_m$  = overall inertial head  
 $L_m$  = equivalent length (inertial)

$$L_m = A'_c \sum_{i=1}^m \frac{L_i}{A_i} \quad (14)$$

for a conduit made up of  $m$  sections of lengths  $L_i$  and areas  $A_i$ .

53. The water-surface differential,  $Z_U - z$ , is the sum of the inertial effect (Equation 13) and the energy losses (Equation 12), or

$$\frac{k_t V_c^2}{2g} = (Z_U - z) - \frac{L_m}{g} \frac{dV}{dt} \quad (15)$$

54. Continuity applies to the culvert flow ( $nA'_c V_c$  where  $n$  is the number of culverts) and the rate of rise  $A_L(dz/dt)$  of the lock chamber water surface giving

$$V_c = \frac{A_L}{nA'_c} \frac{dz}{dt} \quad (16)$$

and

$$\frac{dV}{dt} = \frac{A_L}{nA'_c} \frac{d^2 z}{dt^2} \quad (17)$$

55. Integration of Equation 15 (with  $k_t$  constant and for reasonably high lifts, greater than 5 ft) results in

$$\frac{dV}{dt} \approx \frac{-gnA_c}{k_t A_L} \quad (18)$$

Finally, combining Equation 17 with Equation 18 yields the following expression of  $k_t$  :

$$k_t = \frac{-g \left( \frac{nA'c}{A_L} \right)^2}{\frac{d^2z}{dt^2}} \quad (19)$$

All of these equations relate to lock filling; however, they also apply to emptying, provided appropriate sign changes are applied.

56. Two methods of determining  $k_t$  from experimental data are used here:

- a. Method 1, steady flow. Whenever  $dV/dt$  equals zero and  $Z_U - z$  and  $Q$  are known, then  $k_t$  can be calculated directly from Equation 15.  $dV/dt$  equals zero when the rate of rise reaches its maximum, which is at or near  $t_v$  (Figure 8).
- b. Method 2, rate of rise. Whenever rate of rise  $dz/dt$  is known,  $V$  can be calculated (Equation 16); similarly the slope of this  $dz/dt$  provides a  $dV/dt$  value by means of Equation 17. The value of  $k_t$  can then be calculated by means of Equation 19. The best-fit equations of the prototype  $dz/dt$  for each FE run are shown in Plates 7-10.

The resulting prototype evaluations of  $k_t$  using both Methods 1 and 2 is as follows:

Condition	Test	Method 1			Method 2	
		$V_c$ fps	$Z_U - z$ ft	$k_t$	$d^2z/dt^2$ ft/sec <sup>2</sup>	$k_t$
Filling (two valves)	FE1	45.79	58.97	1.809	-0.00051720	1.860
	FE3	51.40	75.36	1.835	-0.00052054	1.848
	FE9	51.22	72.95	1.789	-0.00052869	1.819
				Avg = 1.81		Avg = 1.84
Filling (one valve)	FE5	53.21	70.60	1.605	-0.00015173	1.585
	FE7	55.74	76.74	1.589	-0.00015300	1.579
				Avg = 1.60		Avg = 1.58
Emptying (two valves)	FE2	41.55	69.47	2.589	0.00033657	2.858
	FE4	39.29	61.97	2.583	0.00030583	3.145
	FE10	40.61	66.89	2.611	0.00031691	3.035
				Avg = 2.59		Avg = 3.01
Emptying (one valve)	FE6	45.50	70.37	2.187	0.00010140	2.372
	FE8	45.87	74.93	2.291	0.00009764	2.463
				Avg = 2.24		Avg = 2.40

The  $k_t$  values for the filling runs compare very well between both methods. There is some slight variation with the emptying runs which can be attributed to inaccuracies in determining  $dV/dt$  for method 2.

Model-prototype correlation  
of basic lock performance

57. A convenient comparison of the relative efficiencies of the model and the prototype is by means of the lock design equation (Equation 5) solving for  $C_L$ . The ideal model-prototype comparison would include the exact duplication of all lock operation variables, i. e., pool elevations and valve times. These varied from the physical model to the prototype, thus requiring some adjustment to the model. This was accomplished with the CORPS program H5322. H5322 was calibrated to the physical model; then the prototype pool elevations and valve times were substituted in the program, giving the physical model predictions of the tested prototype conditions. The resulting model operation times are included in Figure 14. The model values of  $C_L$  were computed as were the prototype values described in paragraphs 48-49. The results are compared as follows:

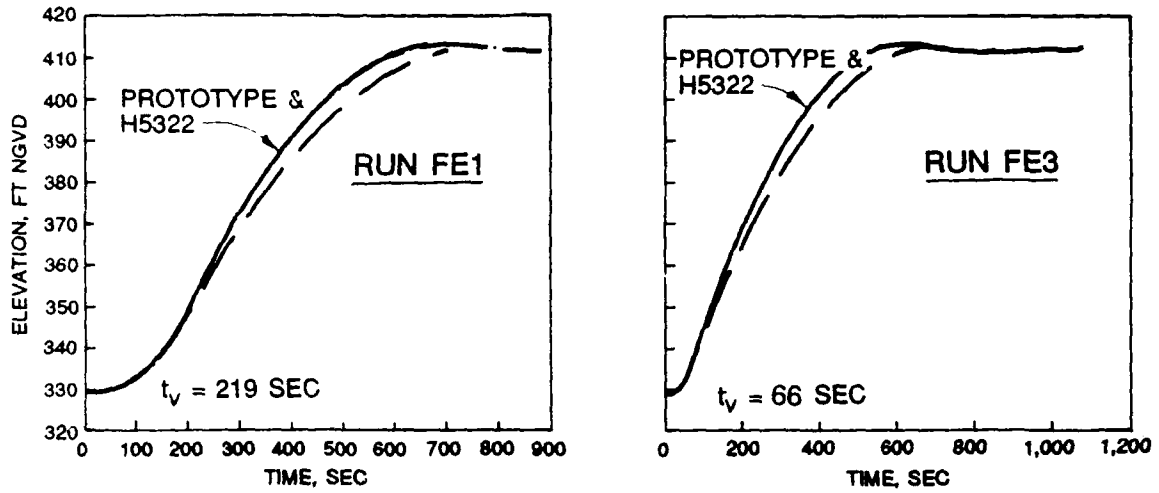
<u>Condition</u>	<u>Model (M) or Proto- type (P)</u>	<u><math>C_L</math></u>	<u><math>k_t</math></u>	<u>Percent Change of Prototype Relative to Model</u>	
				<u><math>C_L</math></u>	<u><math>k_t</math></u>
<u>Filling</u>					
Two-valve	M	0.63	2.52		
	P	0.72	1.81	+14	-28
One-valve	M	0.65	2.37		
	P	0.77	1.60	+18	-32
<u>Emptying</u>					
Two-valve	M	0.52	3.70		
	P	0.58	2.59	+12	-30
One-valve	M	0.55	3.31		
	P	0.64	2.24	+16	-32

58. As shown in this tabulation, the prototype fills and empties more efficiently than the model. The differences in the comparative efficiencies for the various conditions are expected at Bay Springs due to the combined effects of duration of lock operation (single-valve runs are longer) and the

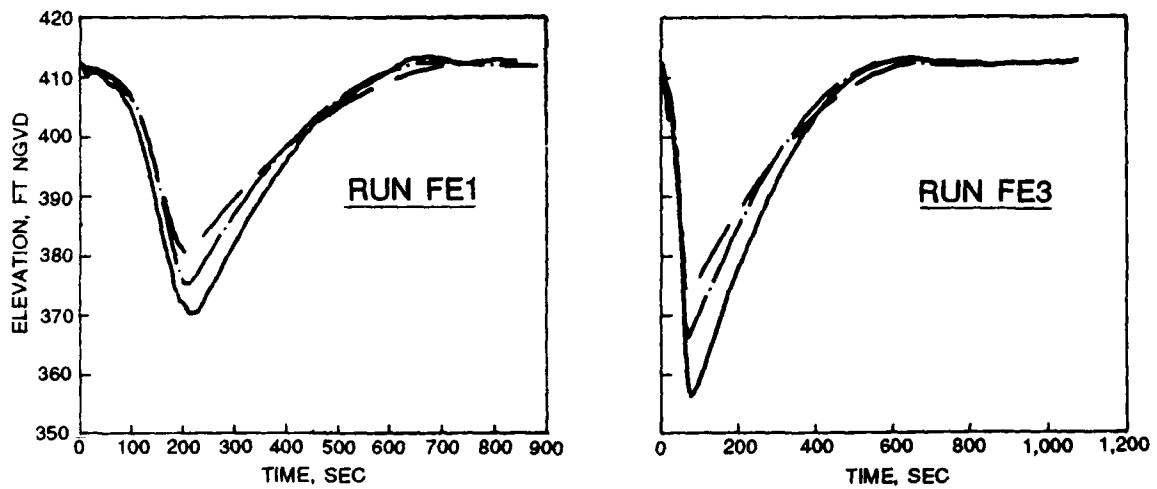
large difference in Reynold's number (R) between the model and prototype.

59. Included in the listing in paragraph 57 is the comparison of the model and prototype values of  $k_t$ . The prototype  $k_t$  values are from the method 1 computations described in paragraph 56. For the model,  $k_t = 1/C_L^2$ . This relationship is evident when the basic formulation for loss coefficients (Equation 16) is equated with the traditional lock coefficient equation (Equations 3 and 4).

60. Figure 16 presents comparisons of the prototype measured values for lock chamber water-surface elevation and filling valve well water-surface elevation with values for both the physical and numerical models. The conditions presented are for two-valve filling at the nominal 1- and 4-min rates. The physical model results were adjusted to prototype conditions as described in paragraph 57 and the numerical model (H5322) calibrated to the prototype according to the measured filling time. As shown, H5322 calculates the filling curve very accurately. For the valve well water-surface elevations, the lowest elevation computed by H5322 is approximately 5 ft higher than that measured in the prototype. The physical model responds as expected (paragraph 58) with a longer filling time and much less drastic valve well response.



a. Lock chamber water-surface elevation



**LEGEND**

PROTOTYPE ———  
 H5322 - - - - -  
 PHYSICAL MODEL - · - · -

b. Valve well water-surface elevation

Figure 16. Model-prototype comparison of basic lock performance

## PART IV: HYDRAULIC CHARACTERISTICS OF THE CULVERTS AND VALVES

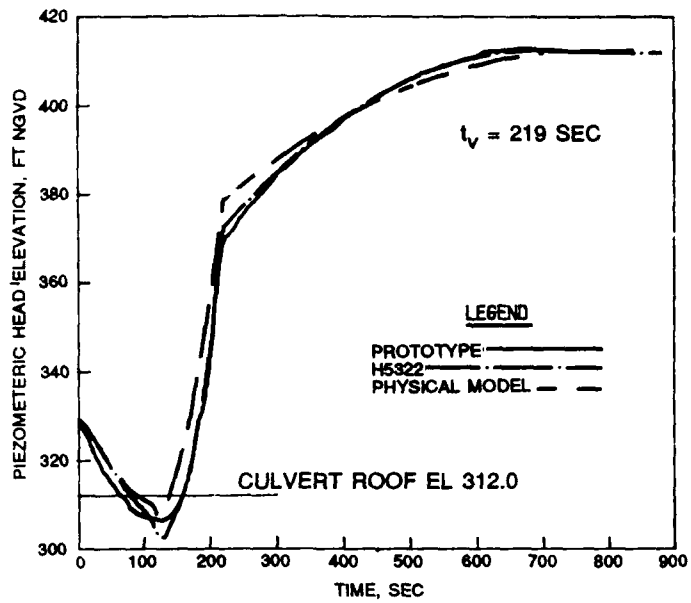
### Culvert Pressures Downstream from Valves

61. Piezometric pressures were measured downstream of the left-wall filling and emptying valves at locations determined to be nearest the point of minimum pressure, or vena contracta. These locations are denoted as LCP1 and LCP5 for the filling and emptying valves, respectively. Plates 1 and 2 show actual locations and Table 1 lists specifics about the transducers. Plates 7-10 present the averaged pressures for the filling and emptying runs. Table 6 lists the mean, instantaneous, and peak-to-peak low pressures. As with the valve well water-surface elevations, the culvert piezometric pressures are used herein to determine certain losses and coefficients for the lock.

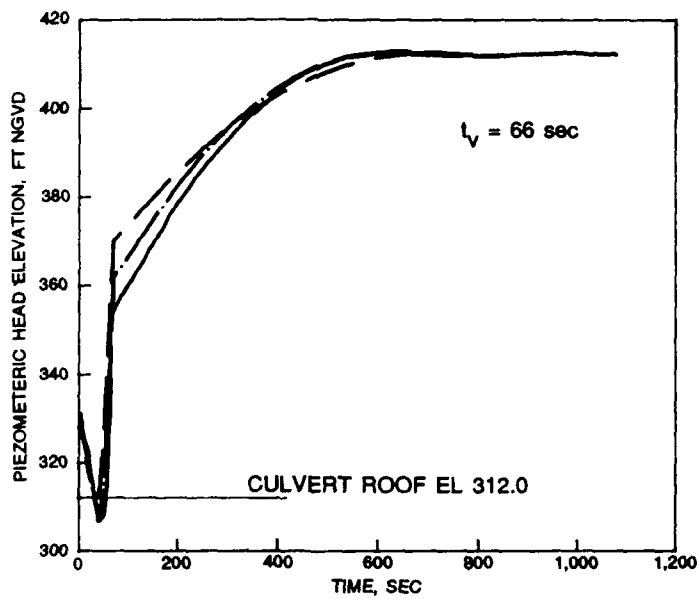
62. Thirty-one feet downstream of LCP1 is transducer LCP2, which is downstream of the valve bulkhead recess (see Plate 2 and Table 1). Typical culvert pressure time-histories are shown in Plate 14. These time-histories give a good indication of the magnitude and intensity of the pressure fluctuations occurring at these locations. The mean, instantaneous, and peak-to-peak low pressures are listed in Table 6 for these transducers. As expected, the mean piezometric pressure at LCP1 fell below that of LCP2 during valve operation and then stayed slightly higher after the valve reached fully open. However, the pressure fluctuations were more intense for location LCP2 than for LCP1. These higher fluctuations were most likely caused by the turbulence created by the bulkhead recess. Cavitation "pops" were noted in the area around the bulkhead slot; however, the severity cannot be quantified with the instrumentation used.

#### Model-prototype comparison

63. Figure 17 presents the model-prototype comparison of the mean pressures acting on the culvert roof at transducer location LCP1. Both the calibrated numerical model (H5322) and the physical model results are shown. The physical model pressures remained substantially higher than the prototype values during valve operation. This is expected of the less efficient model with high relative friction and lower velocities. These further translated into higher loss coefficients (tabulation in paragraph 57) for the physical model. Comparison of H5322 with the prototype revealed lower pressures for



a. Run FE1



LEGEND

PROTOTYPE ———  
 H5322 ———  
 PHYSICAL MODEL - - -

b. Run FE3

Figure 17. Model-prototype comparison of culvert pressure below filling valve

H5322 than for the prototype during valving. The difference was attributed to venting in the prototype. This is most evident in run FE1 in which significant venting occurred during the slow valving (3.65 min) to raise the pressures. For the fast valving, the pressures show little difference. Differences during valving prior to venting (Figure 17, Run FE1) were attributed to valve contraction coefficient  $C_c$  values used in the model. In general, H5322 correlated well with the prototype.

#### Effects of venting

64. An objective of the AV series of tests was to illustrate the significance of airflow on the culvert pressure below the filling valves (LCPI location). The AV tests were conducted with different air vent configurations: (a) with the air vents fully open, (b) with the 6-in. orifice plates installed, and (c) with the vents closed. The resulting pressures are presented in Plates 15 and 16. As expected, the mean pressures were lowered and the pressure fluctuations increased as the airflow was throttled. With the air vents closed, pressures reached dangerously low levels resulting in major cavitation (booming). The severity of the cavitation was much greater during the 4-min than the 1-min valving, as evidenced by hard jolting of the valve and greater intensity and frequency of booming in the 4-min test. No pressure measurements were made for the 4-min valving due to transducer failure during the 1-min valve test (Plate 15).

#### Valve Well Water-Surface Elevations

65. Valve well water-surface elevations were monitored in all valve wells in which a valve was in operation. Filling valve well measurements are shown in Plates 7 and 8; emptying valve well measurements are shown in Plates 9 and 10. The valve wells functioned as piezometers with the water-surface elevations providing a convenient measure of the piezometric heads at the valves. These measurements will be used throughout this portion of the analysis in computing certain losses and coefficients. Listed in Table 6 are the low piezometric heads (valve well water-surface elevations) measured at the valves. These include the mean low pressures, lowest instantaneous pressures, and the greatest peak-to-peak pressures and corresponding frequencies.

### Valve Discharge and Contraction Coefficients

66. Discharge and contraction coefficients were computed using data from the steady-state (SS) series and the incipient airflow and cavitation (CA) series of tests for which no venting occurred. The valve discharge coefficient  $C_d$  is defined (Rouse 1946) as

$$C_d = \frac{BV_c}{b\sqrt{2g\Delta H}} \quad (20)$$

where  $\Delta H$  is the differential piezometric head evaluated across the valve. The velocities are based on a flow rate  $Q$  determined from the rate of rise of the lock water surface. The contraction coefficient  $C_c$  is determined by using Equation 20 and the relationship (Rouse 1946)

$$C_d = \frac{C_c}{\sqrt{1 - C_c^2 (b/B)^2}} \quad (21)$$

Values of the discharge and contraction coefficients as computed using Equations 20 and 21 are listed in the following tabulation. The values are for series CA runs and represent the average of at least four different tests.

$b/B$	$\beta$ deg	$C_d$	$C_c$
0.20	127	0.591	0.581
0.30	124	0.613	0.603
0.40	119	0.624	0.606
0.50	115	0.658	0.625
0.60	110	0.688	0.636
0.70	106	0.769	0.677
0.80	103	0.937	0.744
0.90	98	1.218	0.820

67. The computed values for Bay Springs Lock are compared in Figure 18 with the theoretical, two-dimensional slot solution of von Mises\* and experimentally based values of  $C_c$  determined in the laboratory (Pickering (1981)).

---

\* Maurice James. "Analytical Determination of Contraction Coefficients Using Complex Potential Theory," Memorandum for File, US Army Engineer Waterways Experiment Station, Vicksburg, MS.

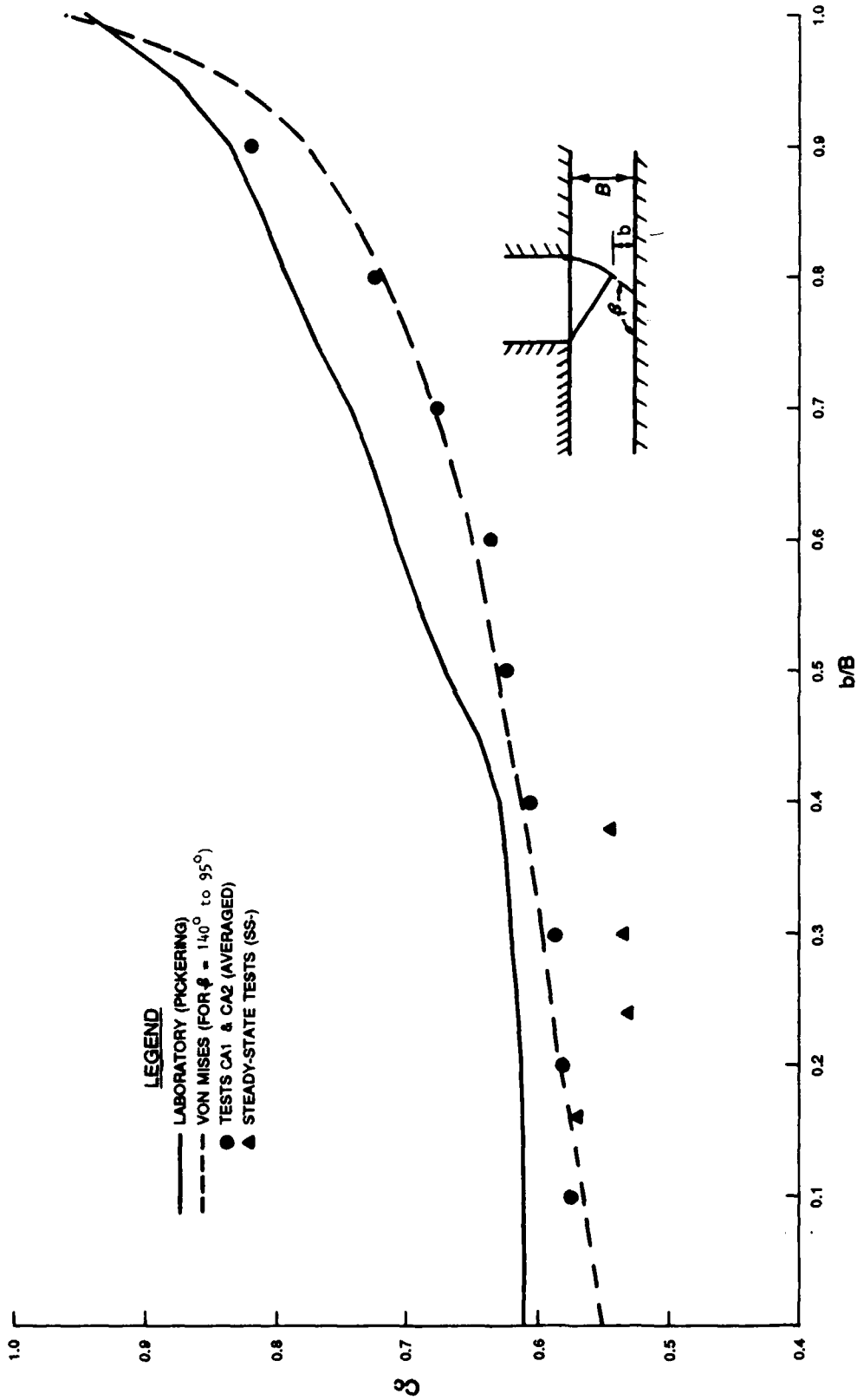


Figure 18. Reverse tainter valve contraction coefficients

The data are in good agreement with the von Mises solution that takes into consideration the angle of the gate lip  $\beta$ . Differences in  $C_c$  between the prototype and both the von Mises and laboratory solutions are attributed to inaccuracies in determining exact values of  $Q$ .

### Cavitation Index

68. The objective of tests CA1 and CA2 was to assess the value  $\sigma_i = 0.6$  used as the parameter for incipient cavitation of unvented reverse tainter valves. The data reduction process compares values calculated by H5322 to field measurements and observations. The analytical relationships are as follows:

$$\underline{\text{Roof pressure } \left( \frac{p}{\gamma_w} \right)_r}$$

$$\left( \frac{p}{\gamma_w} \right)_r = H - Z_r - \frac{(V_c B/C_c b)^2}{2g} \quad (22)$$

$$\underline{\text{Cavitation parameter } \sigma}$$

$$\sigma = \frac{\left( \frac{p}{\gamma_w} \right)_r + 33.0 + (B - C_c b)}{(V_c B/C_c b)^2 / 2g} \quad (23)$$

in which  $Z_r$  is the culvert root elevation in feet and the value -33.0 ft is assumed as vapor pressure (water at 70° F).

The minimum calculated cavitation parameter and the field observations are included in Table 7. Pools and valve times, as listed in Table 2, are input data for each calculation. The vented slow- and fast-valve tests, FE1 and FE3, respectively, with normal initial lock chamber elevations are included for comparison. Plates 17 and 18 present the pressures at LCPI for the CA series of tests. It is beneficial to refer to these plates while reviewing the tables.

69. The LCPI pressure data and the qualitative noises reported in the field notes (Table 7) for the CA test series indicate that an index value of about 0.6 is a reasonable minimum value of the cavitation parameter for the design of submerged reverse tainter valves. For the slow-valve test (CA1) the

value 0.55 denoted minor cavitation, a value of 0.66-0.69 denoted noise but no cavitation, and the value 0.80 denoted very quiet operation. Major cavitation occurred at a value of 0.47. The values for fast-valve operation (CA2 test series) were nearly the same with major cavitation occurring at 0.52 and the point of incipient cavitation computed at 0.64.

70. Significant airflow eliminates the sharp pounding that occurs under unvented conditions. In addition to allowing the flow to be an air-water mixture and therefore inhibiting cavitation damage, venting also raises the minimum pressure downstream of the valve. The minimum calculated unvented pressure and cavitation parameters from H5322 are presented in Plates 19 and 20 with those measured for the normal vented tests (FE series). These plates also illustrate the correlation of airflow with the culvert pressure and cavitation index by noting the times at which the pressure decreased and increased past the culvert roof elevation, venting began and ended, and the pressure reached its lowest. The measured data are listed in Table 8.

71. Cavitation following a vented period, Test FE1 at 3 min, for example (Plate 11), occurred at a cavitation parameter value increasing to about 0.6. The time duration was short so that the design is acceptable; however, raising the valves 6-8 ft would likely have eliminated even this occasional cavitation circumstance. Pulsating airflow, Test CA1-7, for example, that occurs with pressures near zero on the roof downstream from the valve (-2.8 ft in Test CA1-7) does not adequately reduce cavitation pounding.

## PART V: CONCLUSIONS AND RECOMMENDATIONS

### Basic Lock Performance

72. Bay Springs Lock has functioned without major operational problems; in addition, the prototype test data do not indicate any area in which major operational problems might be expected. Following are conclusions based on the analysis of the prototype data regarding the general performance of Bay Springs Lock:

- a. Filling and emptying. The lock filled and emptied satisfactorily for all the valve conditions tested, i.e., single and synchronous, 1- and 4-min nominal valving. As expected, operation times were 70 to 80 percent longer for the single versus synchronous valving. No adverse water-surface conditions existed for either the synchronous or single valving.
- b. Overtravel. Special valving was required to minimize the overtravel. The procedure used at Bay Springs (paragraph 35) virtually eliminated any overtravel.
- c. Valve hoist loads. The tangential forces required to raise the left-wall filling valve were considerably higher than what was predicted. However, they are still less than the available force (Plate 6). The measured hydraulic loads on the tainter valve (hoist loads) were much higher than those predicted by EM 1110-2-1610 (Headquarters, USACE, 1975) (Figure 10). Down-pull loads were as high as 103 kips and at no time were any uplift forces observed.
- d. Air demand. Venting just downstream of all valves at Bay Springs was required to eliminate the damaging cavitation that occurs without adequate venting.
- e. Orifice size. The 6-in.-diam orifice installed on the filling valve air intakes seems to be the optimum size for controlling air entrainment. The pressures were raised such that no damaging cavitation conditions existed. The lock water-surface turbulence caused by the air entrainment posed no hazard to navigation. However, venting with the vents fully open (12-in.-diam opening) caused moderately severe chamber water-surface conditions due to the large quantity of air entrained in the flow, especially for the 4-min valve rate. It is not recommended that Bay Springs be operated with the filling valve vents fully open.
- f. Airflow rates. Air was drawn into the culverts when the valve was between 30 and 80 percent open. Airflow rates were highest for the 4-min nominal valving and for single-valve operations. Observed quantities are shown in Figure 11.
- g. Downstream canal surge. An appreciable surge was generated in the downstream canal during emptying operations. For normal

emptying operations (2-min synchronous valving), the surge height reached 4 ft above normal pool with a maximum rate of rise of 0.07 fps at the center line of the outlet diffuser. At the Mackey's Creek flow control structure, the surge height was reduced by one-half. Wave celerity measured between Bay Springs Lock and Mackey's Creek averaged 24 fps.

- h. Vortex. A 4- to 5-ft wide by 2- to 3-ft deep vortex developed in the approach at Bay Springs during filling operations. The vortex began to form at about 4 min after valving began and lasted approximately 4 min.

#### Hydraulic Characteristics

73. The following parameters of the lock hydraulic system are evaluated in the text:

- a. Culvert discharge coefficient  $C$  (paragraph 46)
- b. Lock coefficient  $C_L$  (paragraph 49)
- c. Valve coefficient  $k$  (paragraph 50)
- d. Overall loss coefficient  $k_t$  (paragraph 56)
- e. Valve discharge coefficient  $C_d$  (paragraph 66)
- f. Valve contraction coefficient  $C_c$  (paragraph 66)

#### Culvert Pressures

74. The culvert pressures just downstream of the valves (transducer LCP1) extended below the culvert roof for all conditions tested. However, sufficient cushioning of these low pressures and pressure fluctuations is provided by venting to prevent any major cavitation booms. Slight cavitation "pops" were measured below the valves just after venting stopped.

75. Just downstream of the bulkhead slot, transducer LCP2 measured mean pressures slightly higher than at LCP1 and pressure fluctuations of higher intensity caused by turbulence created by the bulkhead recess. Cavitation pops were noted in the area of the bulkhead slot. However, the severity could not be quantified with the instrumentation used.

#### Effects of Air Venting on Culvert Pressure

76. Venting allows the flow to be an air-water mixture and therefore inhibits cavitation damage. Venting also raises the minimum pressure

downstream of the valve. The data presented in Plates 15 and 16 illustrate the effects of venting on the pressure acting on the roof of the culvert just downstream of the left-wall filling valve. Without venting, severe cavitation occurred for both the 1- and 4-min valve rates.

#### Cavitation

77. Quantitative measurements of pressures and pressure fluctuations and qualitative measurements of sound at the filling valves provide helpful information in regard to large-scale cavitation pounding.

- a. Tests CA1 and CA2 indicate that an index value of about 0.6 is a reasonable minimum value of the cavitation parameter for the design of submerged reverse tainter valves.
- b. Small cavitation follows the vented periods and occurs at a cavitation parameter value increasing to about 0.6. The time duration is short so that the design is acceptable; however, raising the valves 6-8 ft would likely have eliminated even this occasional cavitation circumstance.

#### Model-Prototype Comparisons

78. Model-prototype comparisons were made throughout the analysis for both the physical model (Ables 1978) and the Corps' numerical model, H5322 (Neilson and Hebler 1988). These comparisons, which include theoretical and established design values, are as follows:

- a. Basic lock performance. As expected, the physical model was less efficient than the prototype. The prototype filled 14 percent faster for two-valve operations and 18 percent faster for one-valve operations. For emptying, prototype operation times were 12 and 16 percent faster for two- and one-valve operations, respectively. The overall loss coefficient  $k_t$  was 30 percent lower for the prototype. These differences are expected and are comparable with other locks.
- b. Culvert pressures. The physical model had lower peak velocities and flow rates and higher critical pressures than the prototype. When calibrated with operation time, H5322 more closely predicted specific items such as extremely low pressures in the culvert system. It is suggested that this analytical approach be used to evaluate such specifics.
- c. Valve coefficients. Computed values of the contraction coefficient  $C_c$  were compared with the theoretical, two-dimensional slot solution of von Mises\* and experimentally

---

\* James, op. cit.

based values determined in the laboratory (Pickering 1981). The data are in good agreement with the von Mises solution that takes into consideration the angle of the gate lip  $\beta$ . The experimental-prototype comparison is reasonable also. Differences are attributed to inaccuracies in determining flow rate in the prototype.

79. Model-prototype comparisons were made for the downstream canal surge for both the physical model (Tate 1978) and the Corps' computer program, H5310 (Neilson 1979). Prototype values for maximum surge height for normal 2-min synchronous valving, measured at the center line of the right outlet diffuser, were higher than the results for both models. The prototype measured 4 ft, the physical model 2.5 ft, and H5310 2.2 ft. The maximum slopes of the water surface, measured as rate of rise, were basically equal.

#### Instrumentation Facilities

80. Several of the proposed measurements for the Bay Springs study had to be eliminated from this test program due to the inability to install instrumentation in the facilities provided. Specifically, pressure measurements were to be made at the beginning of the left-wall splitter plate to determine the balance of flow between the upper and lower portions of the crossover section. This instrumentation consisted of flush-mounted pressure transducers mounted at the nose of the splitter (transducers LDPI and LDP2) and on the upper and lower boundaries (transducers LDP3 and LDP4) as shown in Plate 1. This configuration would effectively convert the splitter into a pitot tube, thus rendering an indication of flow into each section of the crossover. Also, transducer LDP2 was to be used to indicate pressure fluctuations acting on the nose of the splitter pier. This was expected to produce very useful design information. No pull wires were installed, nor was it possible to install them just prior to testing, thus preventing use of the facilities. It is recommended that these facilities be inspected and repaired, allowing for future testing.

81. As mentioned in paragraph 12, transducers LCP3 and LCP4, located in the left-wall filling culvert (Plate 1), were also not instrumented because the transducer mounting box cover plates could not be removed and replaced with the transducer plates. The absence of these measurements prevented the prototype evaluation of valve loss coefficients and culvert resistance

coefficients. These parameters would have contributed significantly to the overall evaluation of the Bay Springs Lock filling and emptying system and to the design of similar systems.

82. It is recommended that all of these facilities be repaired and inspected, allowing for the future testing and evaluation of these important parameters.

## REFERENCES

- Ables, J. H., Jr. 1978 (Nov). "Filling and Emptying System for Bay Springs Lock, Tennessee-Tombigbee Waterway, Mississippi; Hydraulic Model Investigation," Technical Report H-78-19, US Army Engineer Waterways Experiment Station, Vicksburg, MS.
- Headquarters, US Army Corps of Engineers. 1956 (Apr). "Hydraulic Design of Navigation Locks," EM 1110-2-1604, US Government Printing Office, Washington, DC.
- \_\_\_\_\_. 1975 (Aug). "Hydraulic Design of Lock Culvert Valves," EM 1110-2-1610, US Government Printing Office, Washington, DC.
- Howe, J. W. 1950. "Flow Measurement," Engineering Hydraulics, Hunter Rouse, ed., Wiley, New York, pp 202-204.
- Kalinski, A. A., and Robertson, J. M. 1943. "Entrainment of Air in Flowing Water--Closed Conduit Flow," Transactions, American Society of Civil Engineers, Vol 108, pp 1435-1447.
- Neilson, Frank M. 1979 (Apr). "H5310 - Surges in Navigation Channels," Con conversationally Oriented Real-Time Programming System (CORPS), US Army Engineer Waterways Experiment Station, Vicksburg, MS.
- Neilson, Frank M., and Hebler, Martin T. 1988 (Apr). "H5322 - Revision of H5320 WRT Inertia, Hydraulic Friction, Value and Expression," Con conversationally Oriented Real-Time Programming System (CORPS), US Army Engineer Waterways Experiment Station, Vicksburg, MS.\*
- Pickering, G. A. 1981 (Sep). "Lock Culvert Valve Loss Coefficients; Hydraulic Laboratory Investigation," Technical Report HL-81-10, US Army Engineer Waterways Experiment Station, Vicksburg, MS.
- Rouse, H. 1946. Elementary Mechanics of Fluids, Wiley, New York.
- Tate, C. H., Jr. 1978 (Jun). "Bay Springs Canal Surge Study, Tennessee-Tombigbee Waterway, Mississippi and Alabama; Hydraulic Model Investigation," Technical Report H-78-9, US Army Engineer Waterways Experiment Station, Vicksburg, MS.
- US Army Corps of Engineers, "Hydraulic Design Criteria," prepared for Office, Chief of Engineers, by US Army Engineer Waterways Experiment Station, Vicksburg, MS, issued serially since 1952.

---

\* This computer program is available from the Engineering Computer Programs Library, Customer Assistance Group, Information Technology Laboratory, WES.

Table 1

Summary of Instrumentation

Code	Transducer Description		Range	Transducer Location		Sta	El	Cable Length, ft	Refer to Plate	Measurement	Computed Quantity	Comment
	Type	Transducer Feature		Lock Feature	Location							
AV1	Pressure cell	25 psia	Vent intake	2+15.5D	420	1,2			Pressure	Air vent flow rate		
AVR	Pressure cell	25 psia	Vent intake	2+15.5D	420	1,2			Pressure	Air vent flow rate		
DS1	Pressure cell	15 psia	Downstream water surface	8+49D	326.1	1			Pressure	Elevation of water surface		
DS2	Water-level recorder	--	Downstream water surface	89+23.2D	--	--			Elevation	Elevation of water surface		
DS3	Water-level recorder	--	Downstream water surface	272+14.4D	--	--			Elevation	Elevation of water surface		Mackey's Creek min flow structure Lock E pool
GDL	Potentiometer	360° (repeating)	Miter gate	7+47D	424	1			Rotation	Rotation of leaf		
GDM	Potentiometer	360° (repeating)	Miter gate	7+47D	424	1			Rotation	Rotation of leaf		
GSL	Potentiometer	360° (repeating)	Miter gate	0+77D	424	1			Rotation	Rotation of leaf		
GUR	Potentiometer	360° (repeating)	Miter gate	0+77D	424	1			Rotation	Rotation of leaf		
LCP1	Pressure cell	100 psia	Culvert roof	2+33D	312.0	1,2			Pressure	Pressure (average or fluctuation)		
LCP2				2+64D	312.0	1,2						Not installed
LCP3				3+03D	312.0	1						Not installed
LCP4				3+42D	312.0	600						
LCP5				6+13D	312.0	850						
LDP1				3+71.5D	304.0	1,200						
LDP2				3+71.5D	304.5	1,200						
LDP3				3+76.5D	305.0	1,200						
LDP4				3+76.5D	303.0	1,200						
LWSE				4+17D	326.1	550						
MSD	Microswitch	open/closed	Miter gate	7+47D	424	1,000			Open/closed	Time miter gate opens		
MSU	Microswitch	open/closed	Miter gate	0+77D	424	200			Open/closed	Time miter gate opens		
VEL	Potentiometer	360° (repeating)	Valve opening indicator	6+09D	423	750			Rotation	Valve opening		
VER	Potentiometer	360° (repeating)	Valve opening indicator	6+09D	423	1,500			Rotation	Valve opening		
VFL	Potentiometer	360° (repeating)	Valve opening indicator	2+26D	423	275		1,2	Rotation	Valve opening		
VFR	Potentiometer	360° (repeating)	Valve opening indicator	2+26D	423	1,100		1	Rotation	Valve opening		
VHP1	Pressure cell	2,000 psia	Valve cylinder	2+33D	420.5	275		2	Pressure	Cylinder pressure		
VHP2		2,500 psia	Valve cylinder	2+48D	420.5	275		2	Pressure	Cylinder pressure		
WSEL		100 psia	Valve well	5+87D	325.4	750		1				
WSER		100 psia	Valve well	5+87D	326.0	1,600		1				
WSFL		50 psia	Valve well	2+04D	328.1	300		1,2				
WSFR		50 psia	Valve well	2+04D	326.0	1,100		1				
WSI		15 psia	Upstream water surface	0+32U	412.2	300		1				

Table 2  
Test Conditions

Run	Operation	Nominal Valve Opening Rate, min	Type of Valve Operation*	Air Vent Intake Configuration	Upper Pool		Chamber		Lower Pool		Type**
					El	Pool	El	Pool	El	Pool	
FE1	Fill	4	Synchronous	Orifice	412.3	329.3	329.3	329.3	329.3	Allow overtravel	
FE2	Empty	2	Synchronous	Fully open†	412.3	329.4	412.3	329.4	329.4		
FE3	Fill	1	Synchronous	Orifice	412.3	328.9	412.1	328.9	328.9		
FE4	Empty	4	Synchronous	Fully open	412.1	330.4	412.1	330.4	330.4		
FE5	Fill	4	Single valve	Orifice	412.0	330.7	330.7	330.7	330.7		
FE6	Empty	4	Single valve	Fully open	412.2	330.7	412.2	330.7	330.7		
FE7	Fill	1	Single valve	Orifice	412.0	330.7	330.7	330.7	330.7		
FE8	Empty	2	Single valve	Fully open	412.0	330.9	412.0	330.9	330.9		
FE9	Fill	1	Synchronous	Orifice	412.0	330.7	330.7	330.7	330.7		
FE10	Empty	2	Synchronous	Fully open	412.0	330.0	412.0	330.0	330.0		
CA1-1	Fill	4		Orifice	412.2	350.2	350.2	350.2	329.6	Incipient air and cavitation	
CA1-2					412.2	348.2	348.2	348.2			
CA1-3					412.1	346.9	346.9	346.9			
CA1-4					412.1	346.1	346.1	346.1			
CA1-5					412.2	341.2	341.2	341.2			
CA1-6					412.0	337.6	337.6	337.6			
CA1-7					412.0	334.1	334.1	334.1			
CA2-1		1			412.1	342.5	342.5	342.5	330.4		
CA2-2						340.1	340.1	340.1			
CA2-3						343.7	343.7	343.7			
CA2-4						335.2	335.2	335.2			
CA2-5						333.0	333.0	333.0			
CA2-6						332.1	332.1	332.1			
VP-1	Open/Close	4/4	Single valve	N/A	N/A	N/A	N/A	N/A	N/A	Valve cylinder pressures Valve cylinder pressures	
VP-2	Open/Close	1/1	Single valve	N/A	N/A	N/A	N/A	N/A	N/A		
SS-1	Filling valve at 2 ft open			Orifice	412.2	332.4	332.4	332.4	330.4	Steady-state condition	
SS-2	Filling valve at 4 ft open			Orifice	412.2	339.7	339.7	339.7	330.4	Steady-state condition	
SS-3	Filling valve at 5 ft open			Orifice	412.2	345.3	345.3	345.3	329.6	Steady-state condition	
SS-4	Filling valve at 3 ft open			Orifice	412.2	336.3	336.3	336.3	329.6	Steady-state condition	
AV-1	Fill	1	Single valve	Fully open	412.0	330.0	330.0	330.0	330.0	Air venting	
AV-2	Fill	4	Single valve	Fully open	412.0	330.0	330.0	330.0	330.0	Air venting	
AV-3	Fill	1	Single valve	Closed	412.0	330.0	330.0	330.0	330.0	Air venting	
AV-4	Fill	1	Single valve	Closed	412.0	330.0	330.0	330.0	330.0	Air venting	

\* Refer to paragraph 21.

\*\* Refer to paragraph 20.

† Empty valve normal air vent configuration is fully open.

Table 3  
Operation Times

Test No.	Valve Operation		H ft	Operation Times		T, sec Emptying	Overtravel			Miter Gates Opened, sec
	Type	t <sub>v</sub> sec		Filling	T, sec		d <sub>f</sub> ft	t <sub>f</sub> sec	d <sub>e</sub> ft	
FE1	Synchronous	219	83.0	620	--	--	1.5	663	--	639
FE2	Synchronous	118	82.9	--	704	--	--	--	1.0	746
FE3	Synchronous	66	83.4	540	--	--	1.7	619	--	553
FE4	Synchronous	205	81.7	--	767	--	--	--	0.9	819
FE5	Single valve	217	81.3	1,078	--	--	1.1	1,168	--	1,137
FE6	Single valve	207	81.5	--	1,281	--	--	--	0.8	1,367
FE7	Single valve	66	81.3	1,006	--	--	0.9	1,055	--	1,037
FE8	Single valve	126	81.1	--	1,270	--	--	--	0.5	1,350
FE9	Synchronous	67	81.3	532	--	--	0.7	564	--	543
FE10	Synchronous	123	82.0	--	798	--	--	--	0.0	N/A

\* Data channel inoperable, not recorded.

Table 4  
Pool Elevations, Empty Tests

Test No.	Initial Pool El		El at Empty $\Delta H = 0$
	Upper $Z_U$	Lower $Z_L$	
FE2	412.3	329.4	330.0
FE4	412.1	330.4	330.3
FE6	412.2	330.7	330.3
FE8	412.0	330.9	330.5
FE10	412.0	330.0	330.1

Table 5  
Downstream Approach Channel Surge

Test No.	Valves No.	Nominal Rate, min	Data Location*	Downstream Approach El			Surge Height ft	Maximum Water-Surface Rate of rise fps**
				Test Begin	Surge Begin	Surge Peak		
FE2	2	2	DS1	329.4	329.4	332.8	3.4	0.039
			DS2	329.7	329.7	332.1	2.4	--
			DS3	329.9	330.0	330.5	0.5	--
FE4	2	4	DS1	330.4	330.4	333.6	3.2	0.020
			DS2	330.3	330.5	332.1	1.6	--
			DS3	330.0	330.2	330.7	0.6	--
FE6	1	4	DS1	330.7	330.7	331.9	1.2	0.007
			DS2	330.7	330.6	331.6	1.0	--
			DS3	330.4	330.5	330.9	0.4	--
FE8	1	2	DS1	330.9	330.9	332.2	1.3	0.013
			DS2	330.7	330.7	331.7	1.0	--
			DS3	330.4	330.5	330.8	0.3	--
FE10	2	2	DS1	330.0	330.0	334.0	4.0	0.070
			DS2	330.4	330.1	332.2	2.1	--
			DS3	330.5	330.4	330.9	0.5	--

\* Gate stations: DS1 at sta 1+11, center-line diffuser, right side.  
 DS2 at sta 89+23.2, Mackey's Creek.  
 DS3 at sta 271+92.0, Lock E pool.

\*\* -- = time scale used for prototype measurements precludes the accurate determination of rate of rise.

Table 6  
Critical Piezometric Pressures

Test No.	Item*	Transducer Station				
		WSFL	WSFR	LCPI	LCP2	LCP5
FE1	M	369.6	369.5	305.3	308.6	--
	L	367.4	367.0	294.4	287.0	--
	P/P	17.9	28.1	47.6	54.9	--
	F	1.2	1.2	0.8	0.8	--
FE2	M	--	--	--	--	307.1
	L	--	--	--	--	304.3
	P/P	--	--	--	--	13.2
	F	--	--	--	--	2.5
FE3	M	356.4	357.7	305.8	312.4	--
	L	354.9	356.2	303.3	292.8	--
	P/P	6.6	7.0	15.6	28.9	--
	F	1.5	2.0	0.8	1.3	--
FE4	M	--	--	--	--	307.4
	L	--	--	--	--	299.9
	P/P	--	--	--	--	19.4
	F	--	--	--	--	1.8
FE5	M	350.5	--	297.3	301.6	--
	L	349.3	--	295.8	291.5	--
	P/P	9.0	--	27.1	36.0	--
	F	2.0	--	2.0	1.5	--
FE6	M	--	--	--	--	305.4
	L	--	--	--	--	303.3
	P/P	--	--	--	--	25.6
	F	--	--	--	--	1.8
FE7	M	342.2	--	303.2	310.9	--
	L	340.9	--	300.9	294.9	--
	P/P	4.3	--	21.5	37.1	--
	F	1.3	--	1.3	1.0	--
FE8	M	--	--	--	--	307.6
	L	--	--	--	--	305.7
	P/P	--	--	--	--	23.4
	F	--	--	--	--	1.5

(Continued)

Note: -- indicates that data were not pertinent.

\* M = Average low pressure, ft NGVD.

L = Lowest instantaneous pressure, ft NGVD.

P/P = Greatest peak-to-peak pressure, ft of water.

F = Frequency of peak-to-peak pressure, cps.

Table 6 (Concluded)

Test No.	Item	Transducer Station				
		WSFL	WSFR	LCPI	LCP2	LCP5
FE9	M	353.7	359.3	308.4	312.6	--
	L	352.1	358.2	305.3	285.3	--
	P/P	11.6	7.9	26.8	39.1	--
	F	1.5	1.5	1.5	0.8	--
FE10	M	--	--	--	--	307.7
	L	--	--	--	--	306.3
	P/P	--	--	--	--	17.6
	F	--	--	--	--	1.0

Table 7  
Cavitation Index

Test	Valve Opening Ratio b/B	H*	Water Velocity V fps	Contraction Coefficient C <sub>c</sub>	Culvert Roof Pressure (p/γ) ft w/r	Cavitation Parameter σ	Field Notes
FE1	0.438	408.43	3.33	0.642	-10.5	0.30	Vented slow-valve test
CA1-1		409.13	9.95		19.1	0.80	Very quiet; no airflow
CA1-2		409.04	0.27		16.3	0.74	Aborted; operator error
CA1-3		408.90	0.48		14.5	0.70	Noise, no booms; no airflow
CA1-4		408.97	20.63		13.3	0.67	Noise, no booms; no airflow
CA1-5		408.78	21.44		6.4	0.55	Minor cavitation, noise; no airflow
CA1-6		408.45	21.99		1.4	0.47	Severe cavitation booms; no airflow
CA1-7		408.36	22.39		-2.2	0.42	Pulsating airflow; cavitation booms after airflow to b/B = 0.6 (about)
Valve Time = 66 sec							
FL3	0.397	405.00	19.84	0.628	-4.1	0.39	Vented fast-valve test
CA2-1		405.70	17.95		13.1	0.70	Noise, no booms; no airflow
CA2-2		405.50	18.29		9.8	0.64	Incipient cavitation, small booms; no airflow
CA2-3		405.70	17.78		14.7	0.74	Quiet operation; no airflow
CA2-4		405.20	18.97		3.2	0.52	Severe cavitation booms; no airflow
CA2-5		405.10	19.27		0.2	0.47	Pulsating airflow; popping before and after airflow
CA2-6		405.00	19.39		-1.0	0.45	Significant airflow; no cavitation

\* H is the total head in the flow immediately upstream from the valve, ft NGVD.

Table 8  
Culvert Pressure, Airflow, and Cavitation Index Comparison  
Valve Opening Sequence

Test No.	Sequence*	t, sec	b/B	$\left(\frac{P}{\gamma_w}\right)_r$ , ft NGVD	$\sigma^{**}$
FE1 (Fill)	A	69	0.24	312.0	0.59
	B	85	0.29	310.7	0.55
	C	126	0.50	307.1	0.50
	D	166	0.72	314.8	0.60
	E	157	0.67	312.0	0.56
FE2 (Empty)	A	45	0.25	312.0	0.67
	B	52	0.32	310.0	0.66
	C	78	0.54	307.1	0.61
	D	109	0.86	311.0	0.70
	E	110	0.88	312.0	0.72
FE3 (Fill)	A	31	0.36	312.0	0.67
	B	31	0.36	312.0	0.67
	C	42	0.55	305.8	0.54
	D	56	0.80	313.5	0.60
	E	55	0.78	312.0	0.59
FE4 (Empty)	A	77	0.25	312.0	0.63
	B	78	0.26	311.4	0.62
	C	134	0.54	307.4	0.56
	D	171	0.75	311.8	0.63
	E	180	0.77	312.0	0.64
FE5 (Fill)	A	65	0.21	312.0	0.80
	B	79	0.27	308.2	0.66
	C	154	0.66	297.3	0.31
	D	190	0.87	312.0	0.43
	E	190	0.87	312.0	0.43
FE6 (Empty)	A	79	0.27	312.0	0.69
	B	--†	--†	--†	--†
	C	143	0.59	305.4	0.52
	D	188	0.86	311.9	0.63
	E	191	0.89	312.0	0.70

(Continued)

Note: Refer to Plates 19-20.

\* A = Piezometric pressure 312.0 ft NGVD (culvert roof elevation) and decreasing.

B = Start of venting.

C = Average low piezometric pressure on culvert roof, ft NGVD.

D = End of venting.

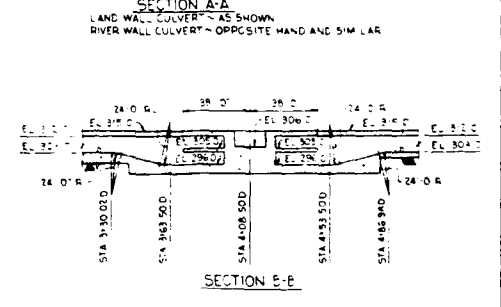
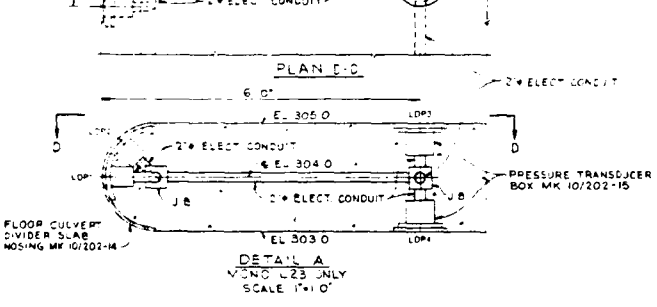
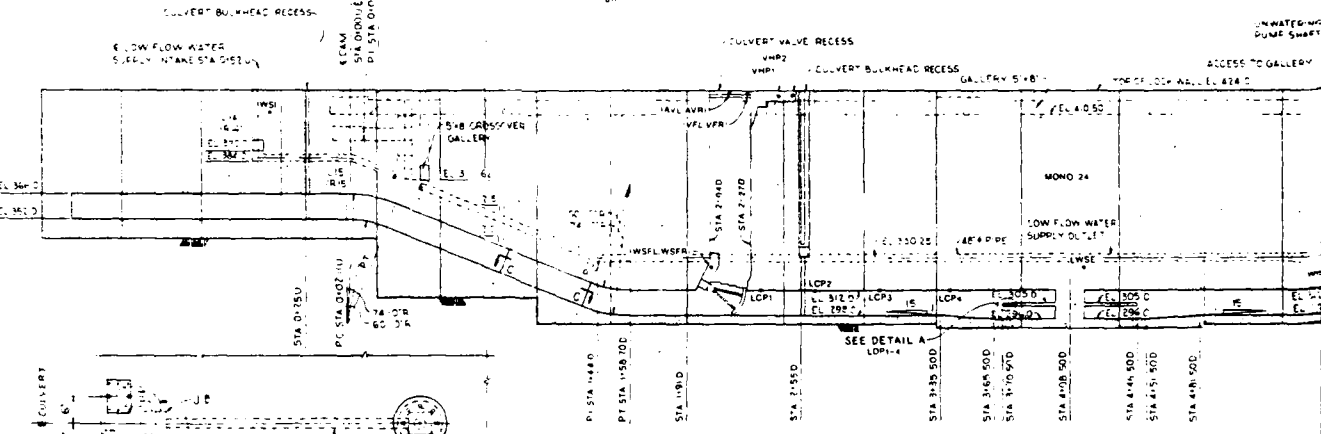
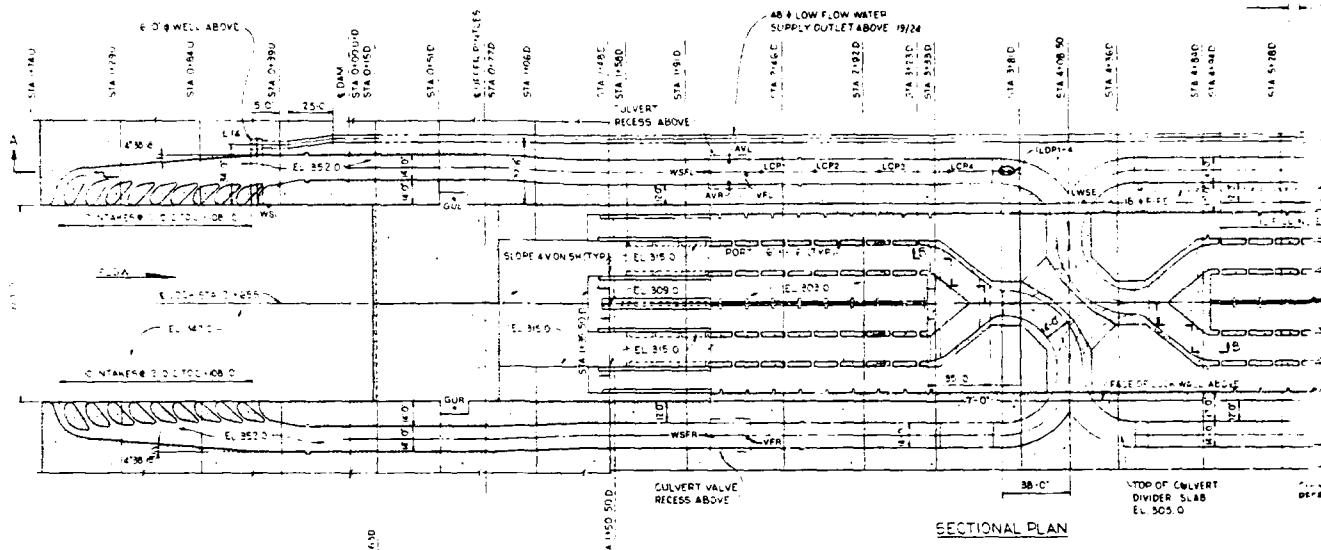
E = Piezometric pressure 312.0 ft NGVD and increasing.

\*\* Computed using von Mises'  $C_c$ .

† Data not recorded.

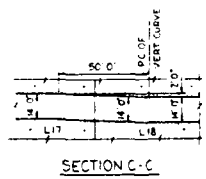
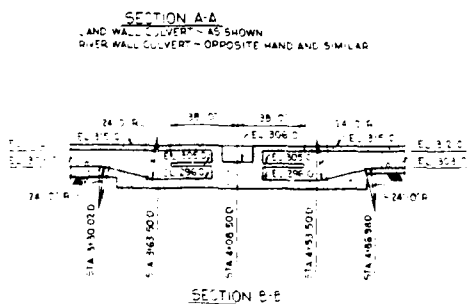
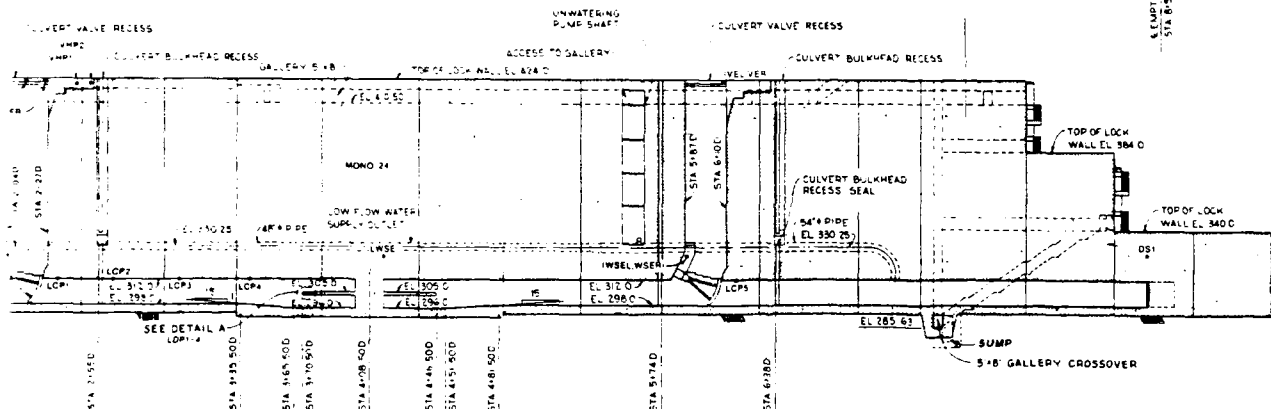
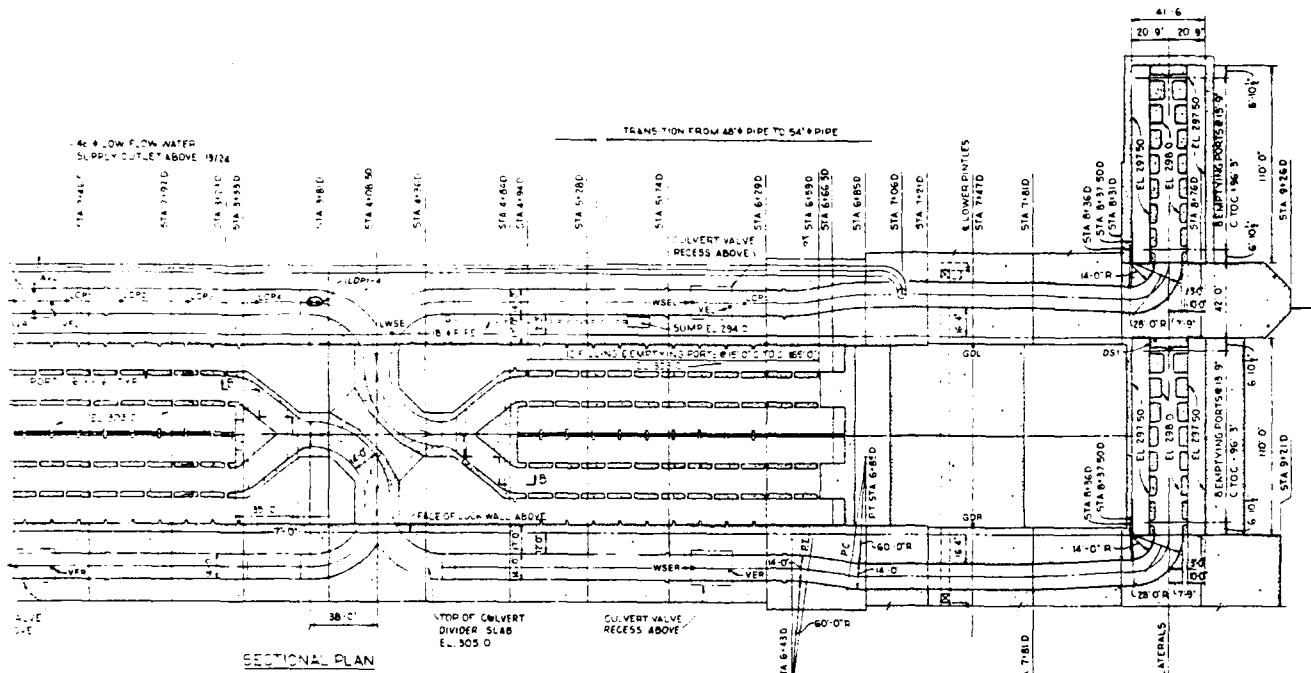
Table 8 (Concluded)

<u>Test No.</u>	<u>Sequence</u>	<u>t , sec</u>	<u>b/B</u>	<u><math>(P/\gamma_w)_r</math> , ft NGVD</u>	<u><math>\sigma^{**}</math></u>
FE7 (Fill)	A	29	0.31	312.0	0.55
	B	32	0.37	310.9	0.50
	C	52	0.70	303.2	0.45
	D	60	0.86	312.9	0.54
	E	58	0.83	312.0	0.49
FE8 (Empty)	A	53	0.29	312.0	0.68
	B	54	0.30	312.3	0.68
	C	90	0.59	307.6	0.59
	D	116	0.88	313.2	0.71
	E	114	0.83	312.0	0.61
FE9 (Fill)	A	35	0.42	312.0	0.71
	B	37	0.45	311.8	0.66
	C	42	0.54	308.4	0.63
	D	56	0.78	314.0	0.66
	E	53	0.74	312.0	0.63
FE10 (Empty)	A	48	0.28	312.0	0.65
	B	54	0.32	310.5	0.63
	C	78	0.53	307.7	0.60
	D	111	0.85	313.3	0.71
	E	110	0.82	312.0	0.69



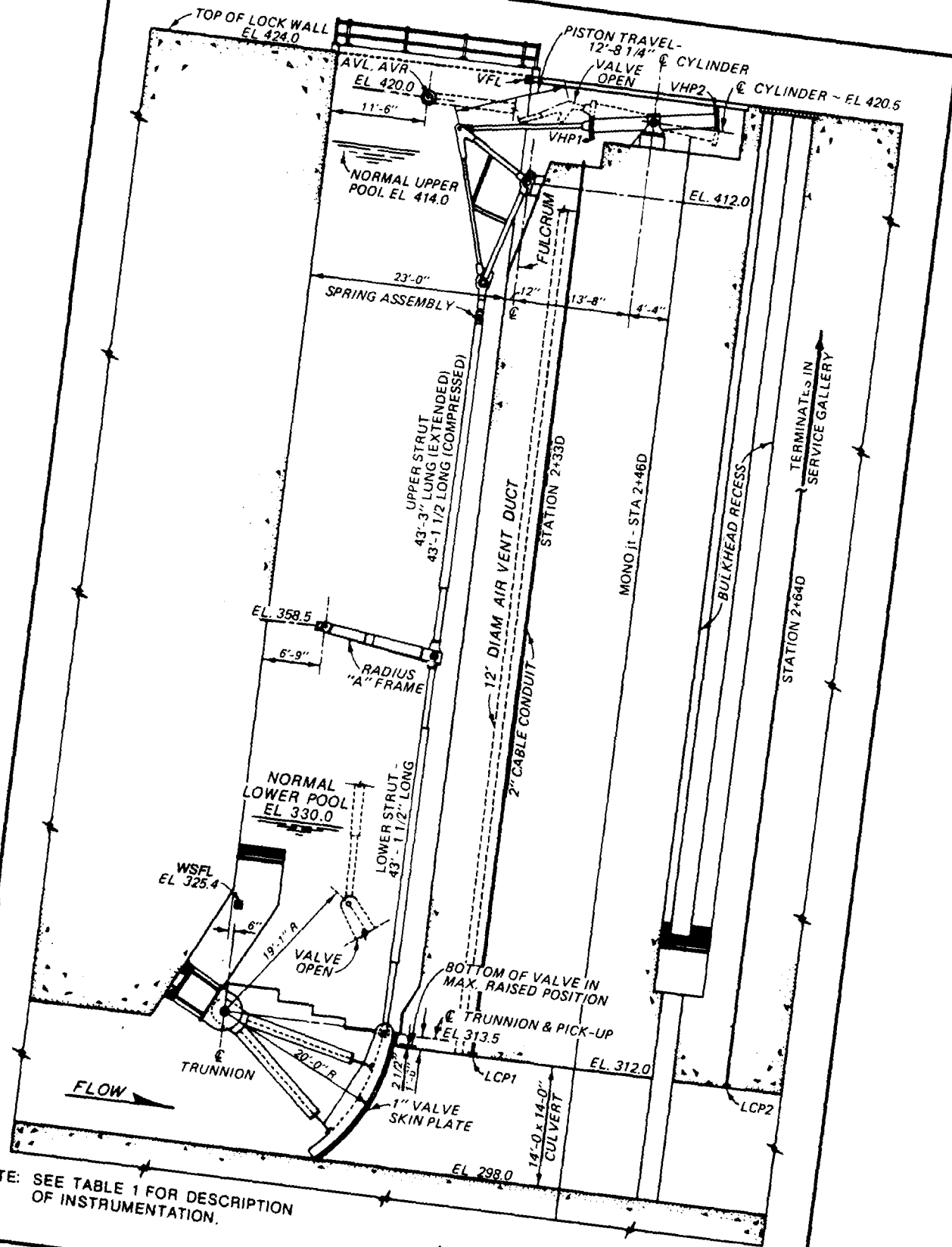
NOTE: See Table 1 for descriptions of instrumentation.

1/3



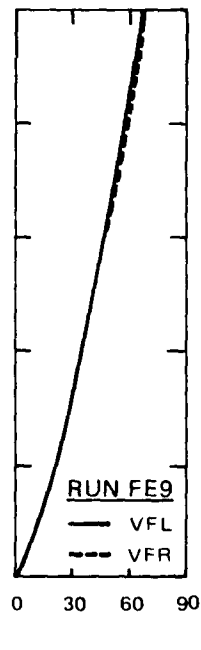
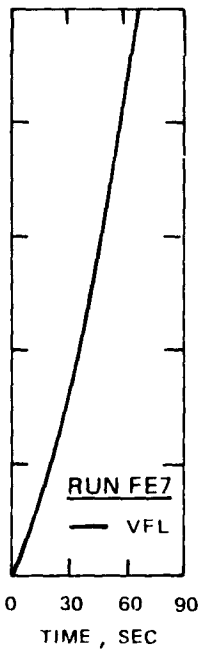
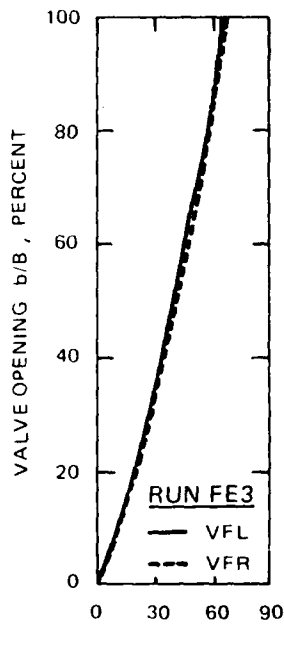
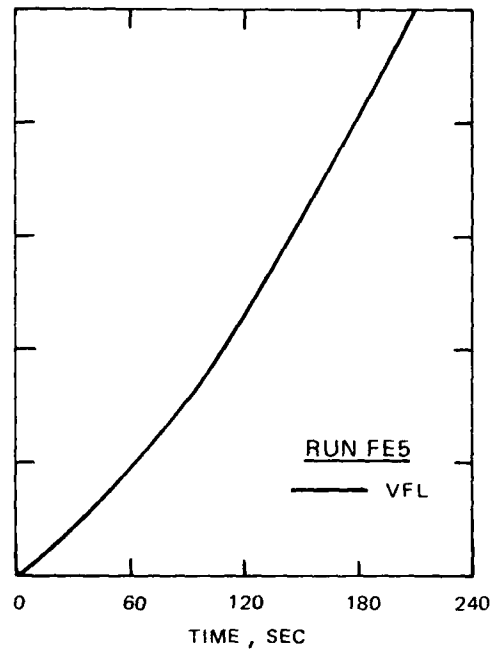
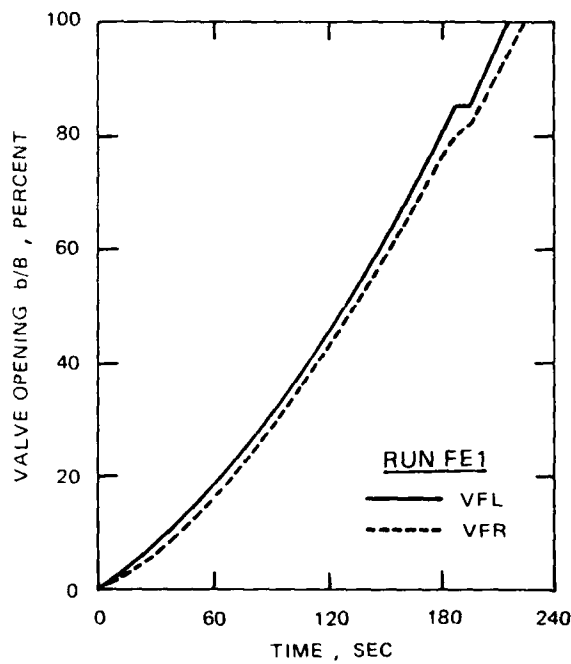
**FILLING AND EMPTYING SYSTEM  
SECTIONAL PLAN AND ELEVATION**

*J. J. J.*

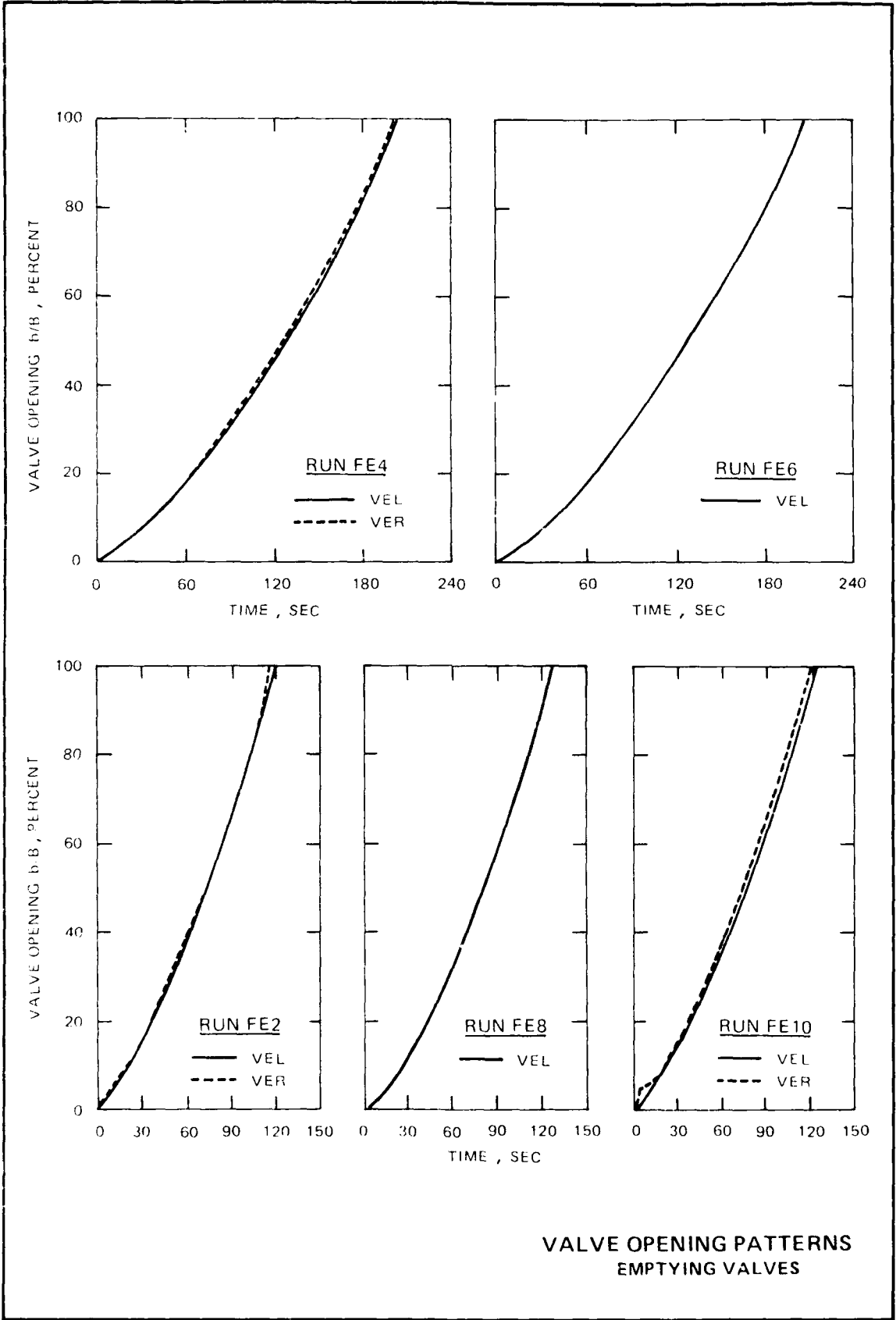


NOTE: SEE TABLE 1 FOR DESCRIPTION OF INSTRUMENTATION.

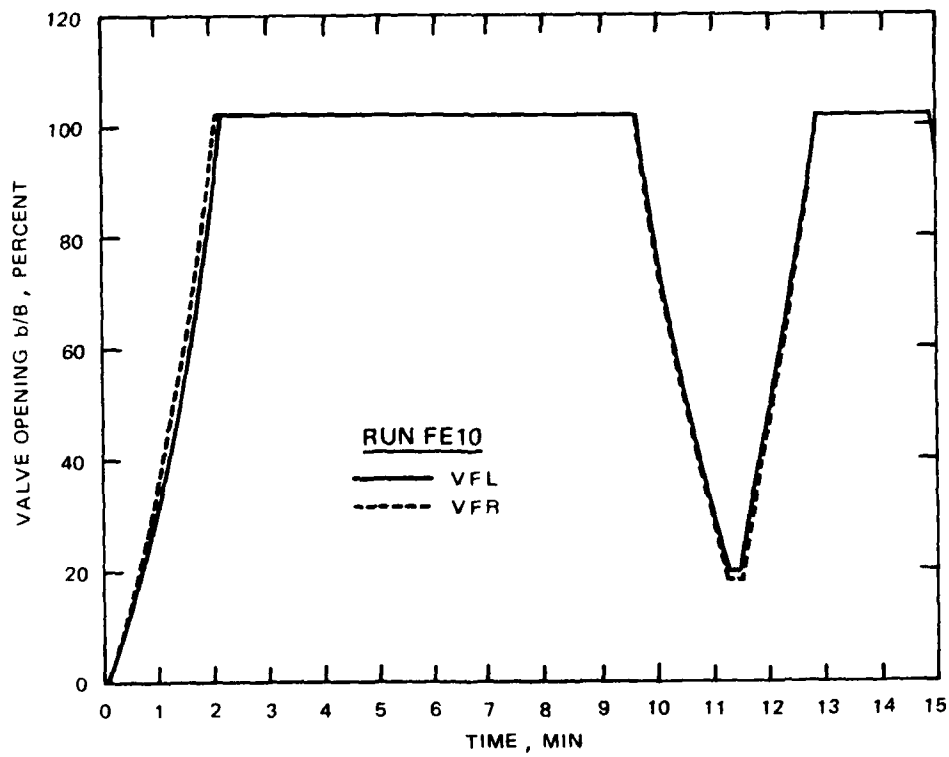
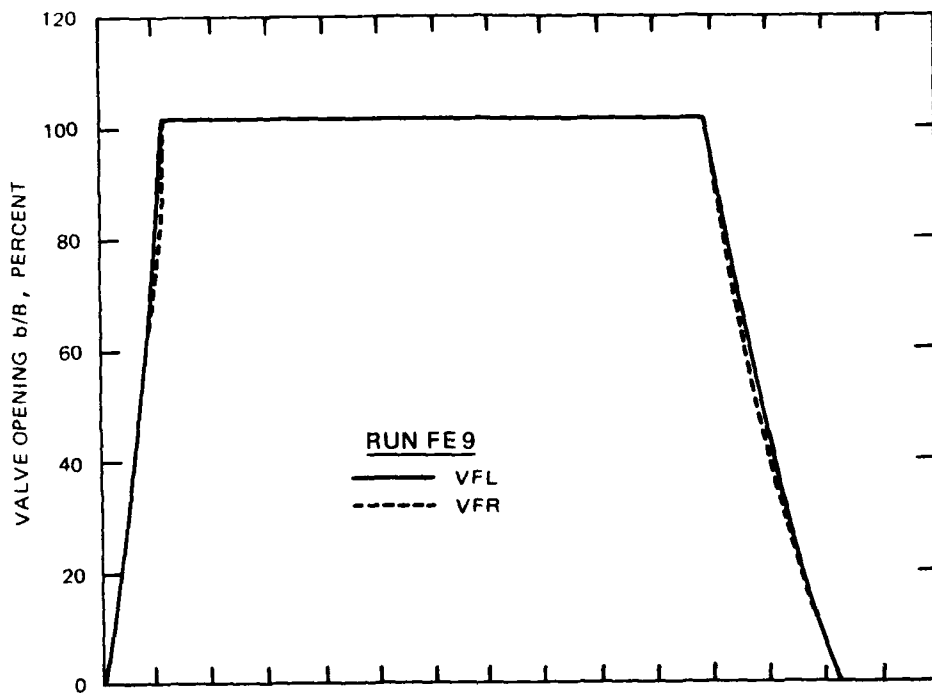
LEFT CULVERT FILLING VALVE



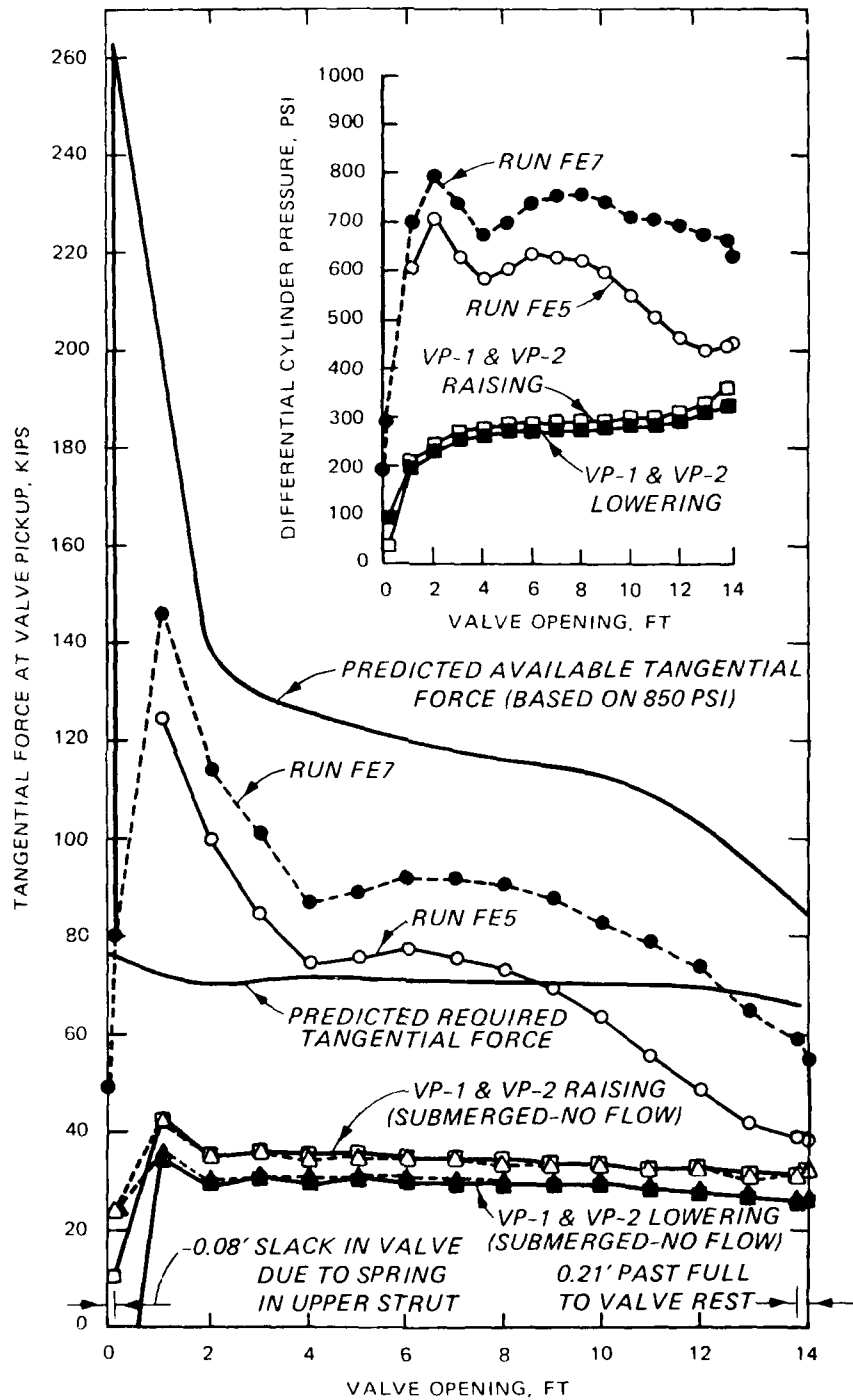
**VALVE OPENING PATTERNS  
FILLING VALVES**



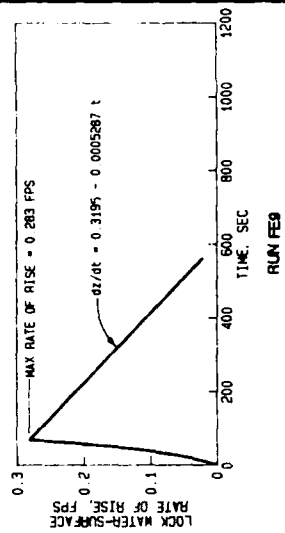
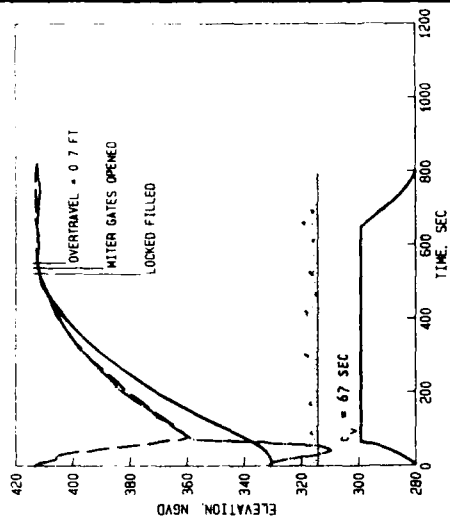
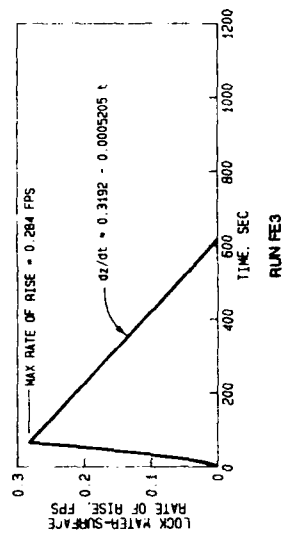
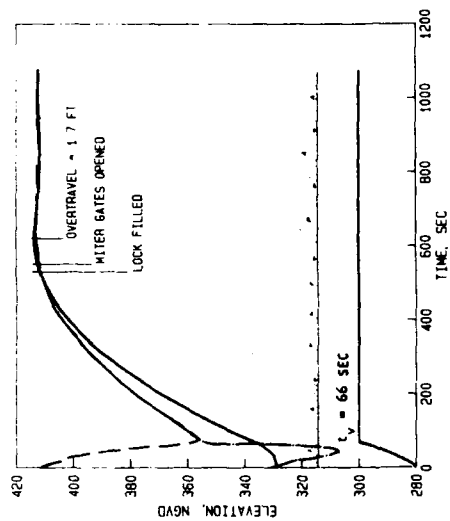
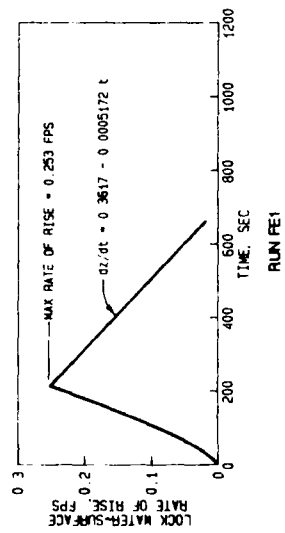
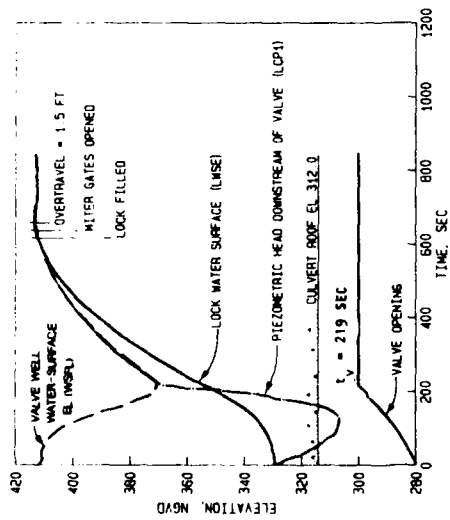
VALVE OPENING PATTERNS  
EMPTYING VALVES



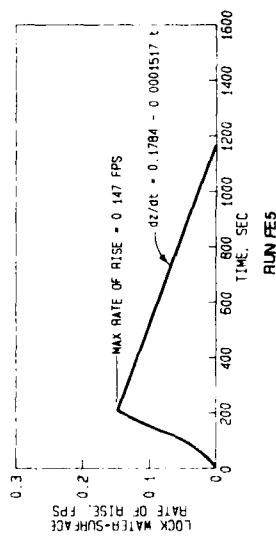
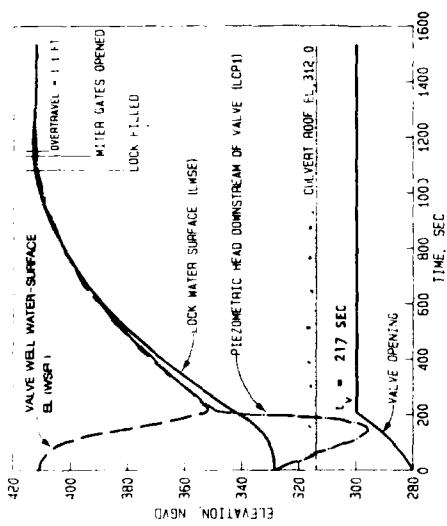
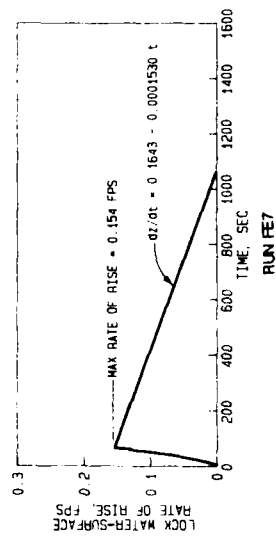
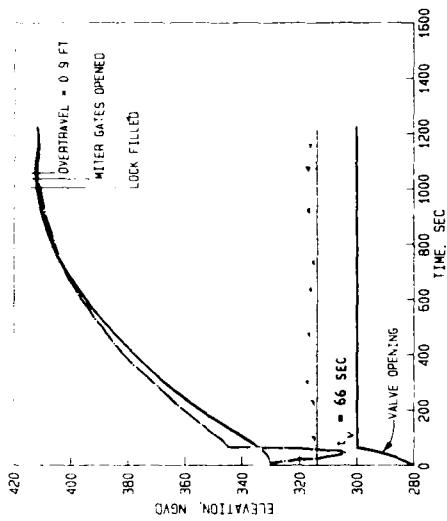
**VALVE PATTERNS  
NORMAL OPERATIONS**



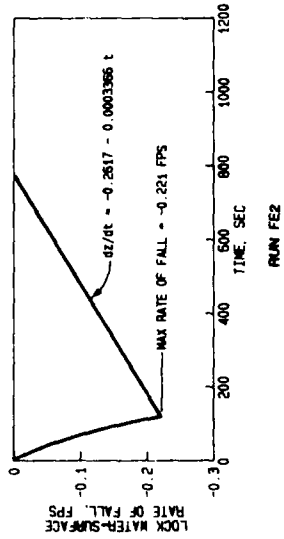
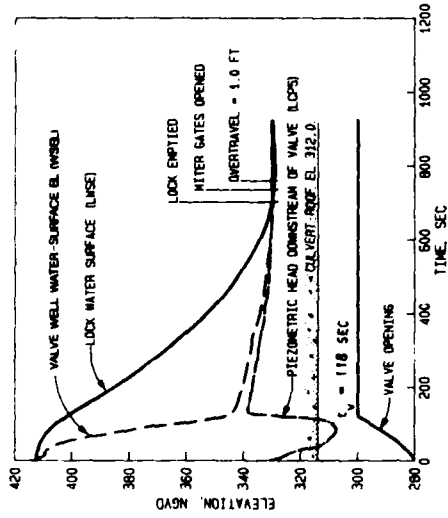
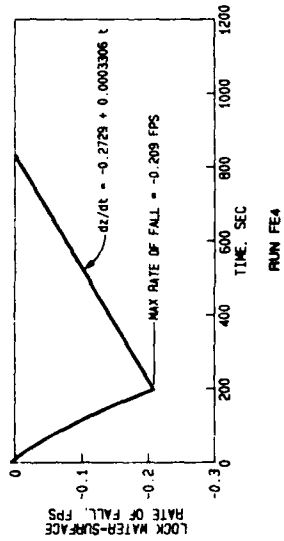
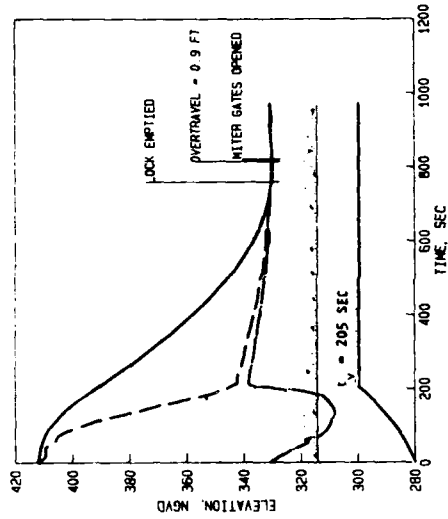
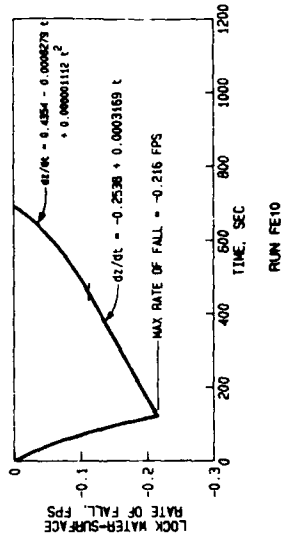
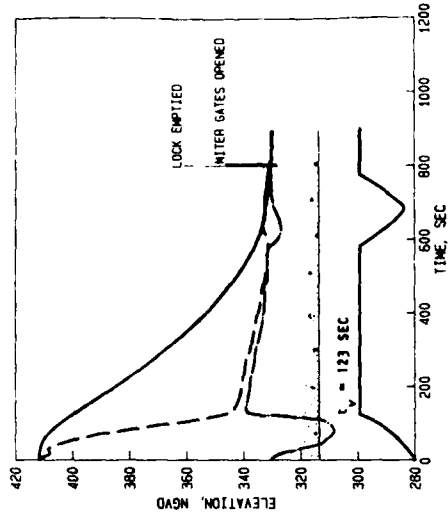
VALVE CYLINDER PRESSURE AND FORCE



WATER-SURFACE ELEVATIONS  
 AND CULVERT PRESSURES  
 TWO-VALVE FILLING OPERATION



**WATER SURFACE ELEVATIONS  
 AND CULVERT PRESSURES  
 ONE-VALVE FILLING OPERATION**

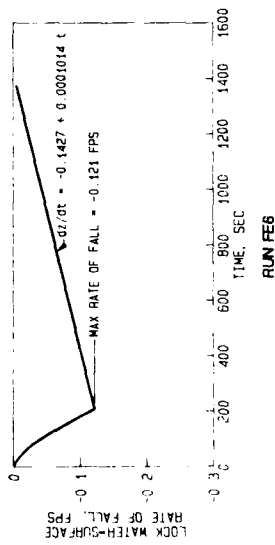
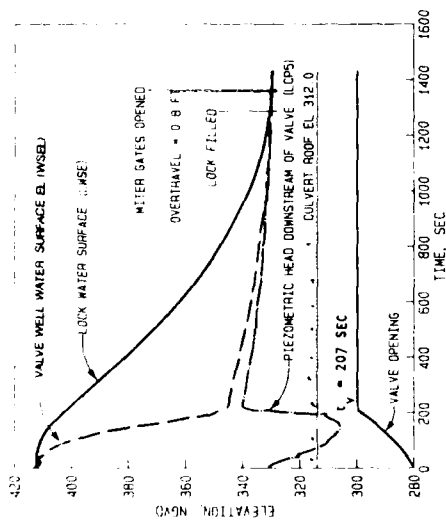
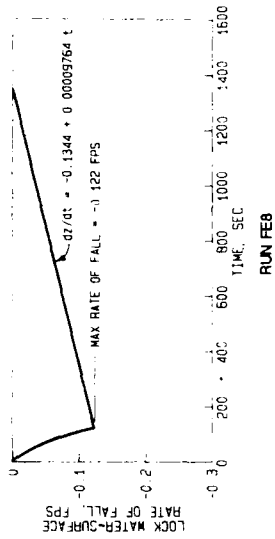
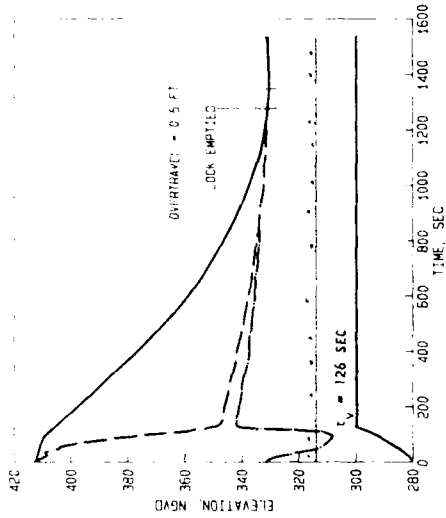


WATER-SURFACE ELEVATIONS  
AND CULVERT PRESSURES  
TWO-VALVE EMPTYING OPERATION

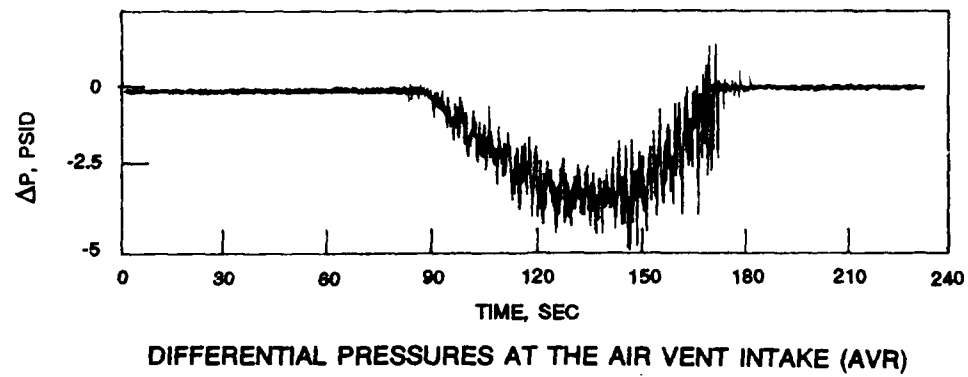
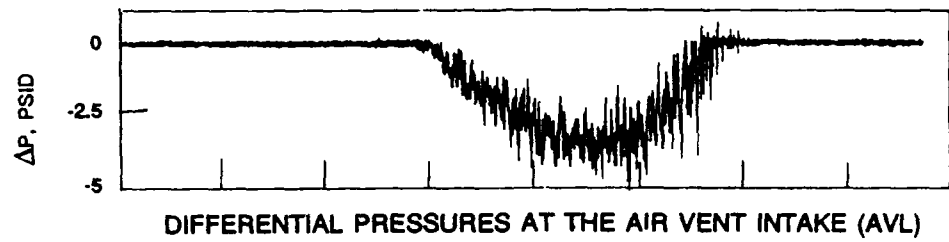
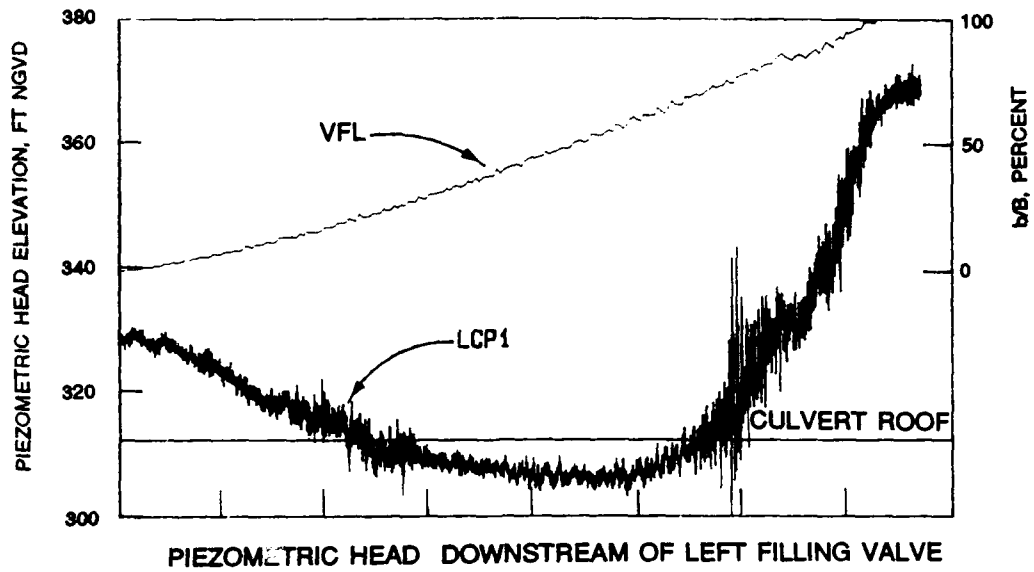
RUN FE10

RUN FE4

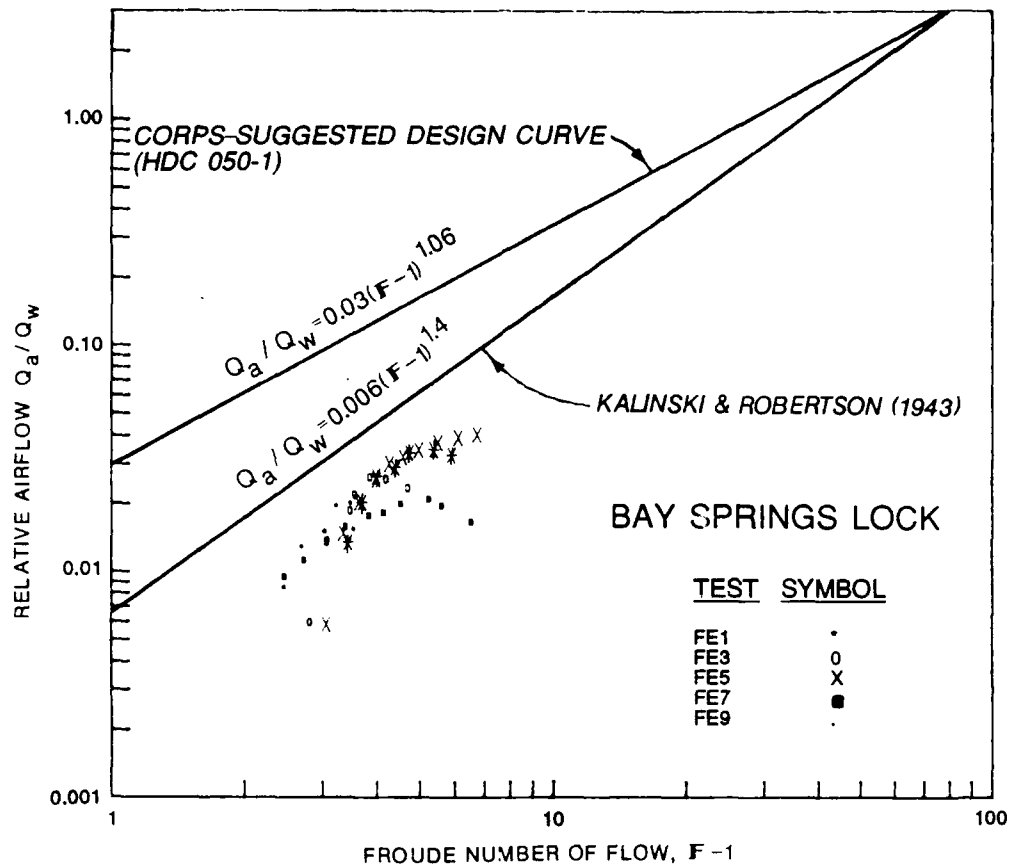
RUN FE2



WATER-SURFACE ELEVATIONS  
 AND CULVERT PRESSURES  
 ONE-VALVE EMPTYING OPERATION

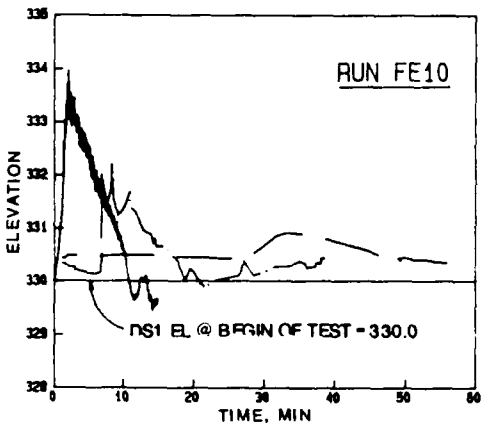
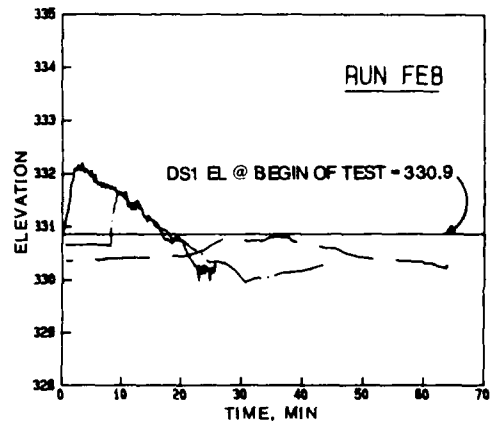
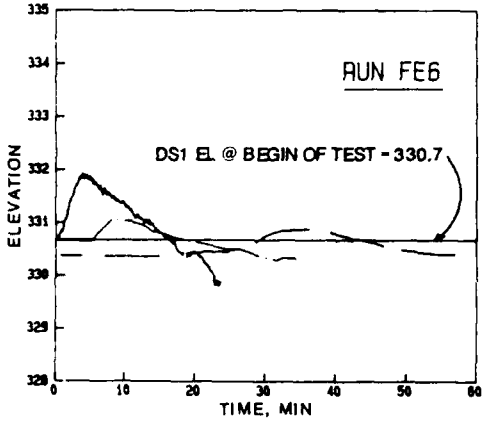
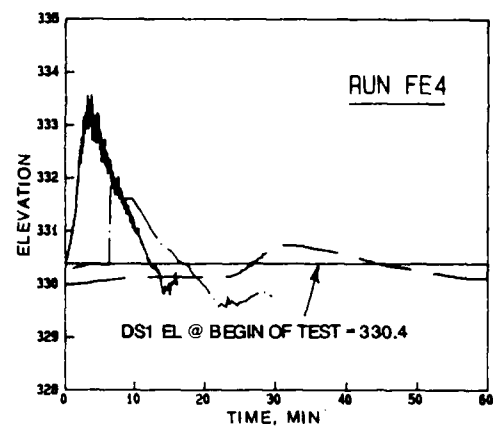
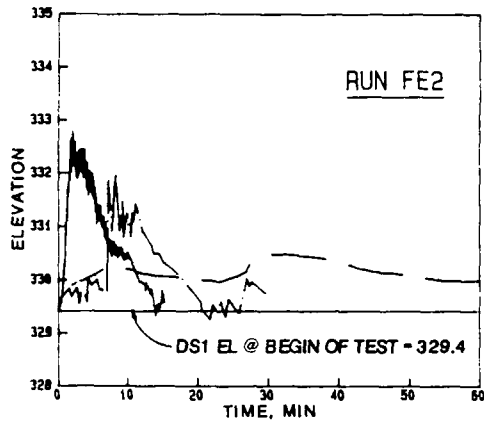


**TYPICAL AIRFLOW  
TIME-HISTORIES**  
RUN FE1



NOTE: ALL DATA MEASURED WITH 6-IN. ORIFICE

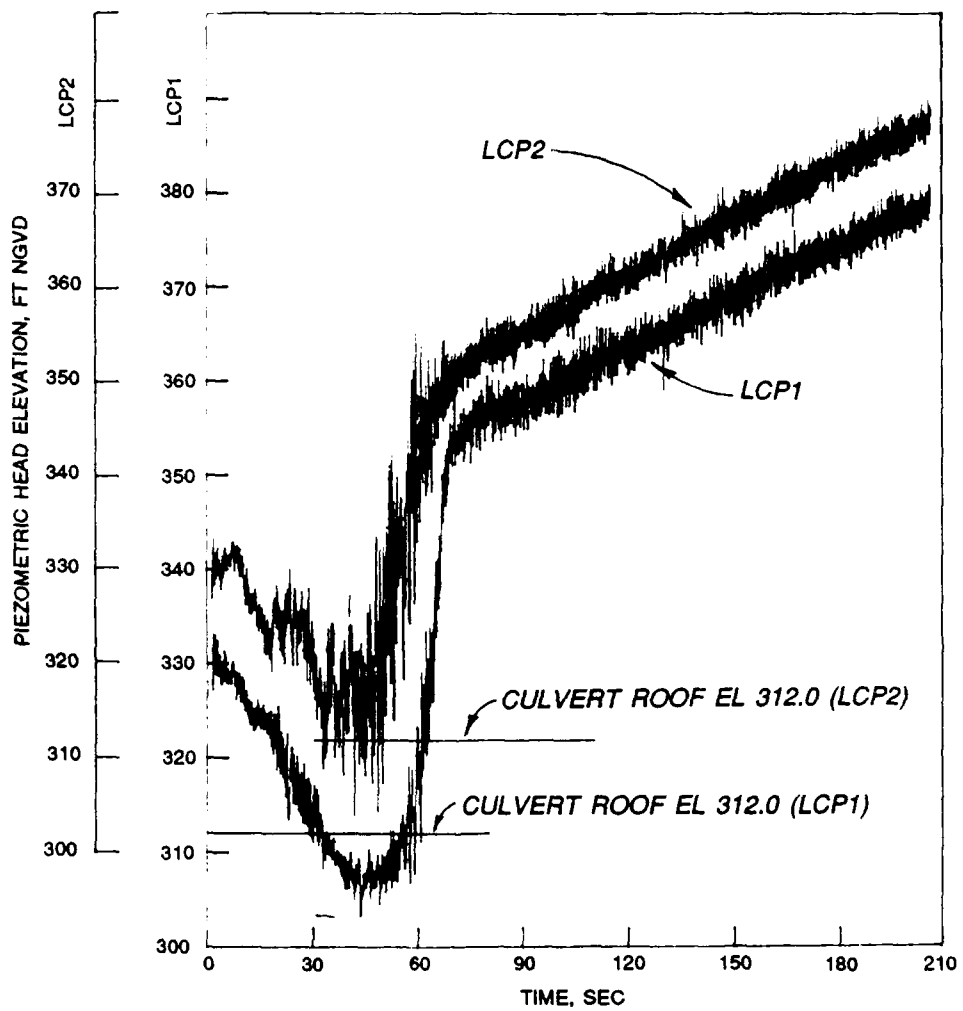
**AIR DEMAND  
FROM HDC 050-1**



**LEGEND**

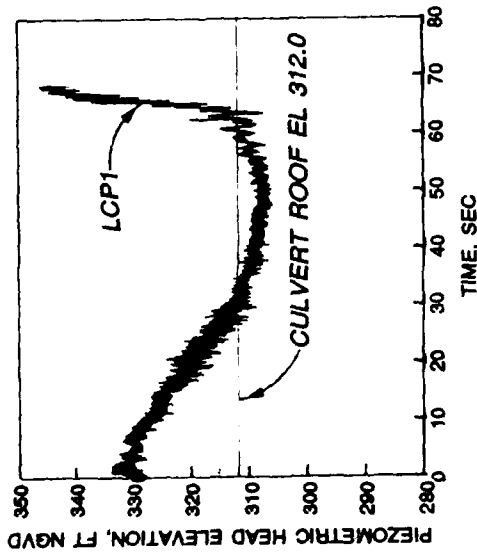
- DS1 ———
- DS2 - - -
- DS3 - - -

DOWNSTREAM SURGE

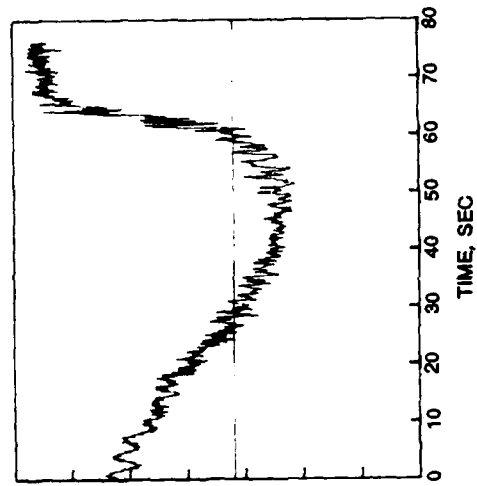


NOTE: CURVE LCP2 IS OFFSET  
VERTICALLY BY 10 FT.

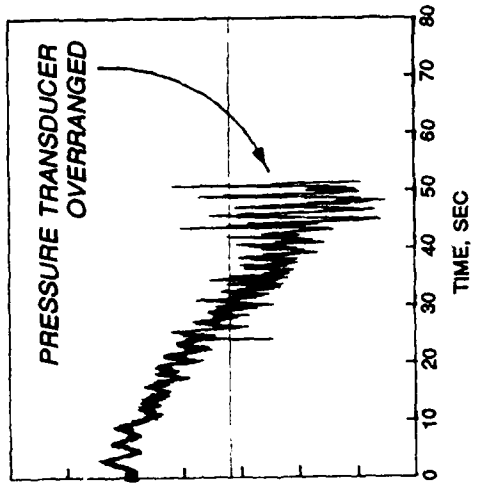
**CULVERT PIEZOMETRIC PRESSURES  
RUN FE3**



RUN AV-1: AIR VENTS FULLY OPEN



RUN FE7: VENTING WITH 6-IN. ORIFICE

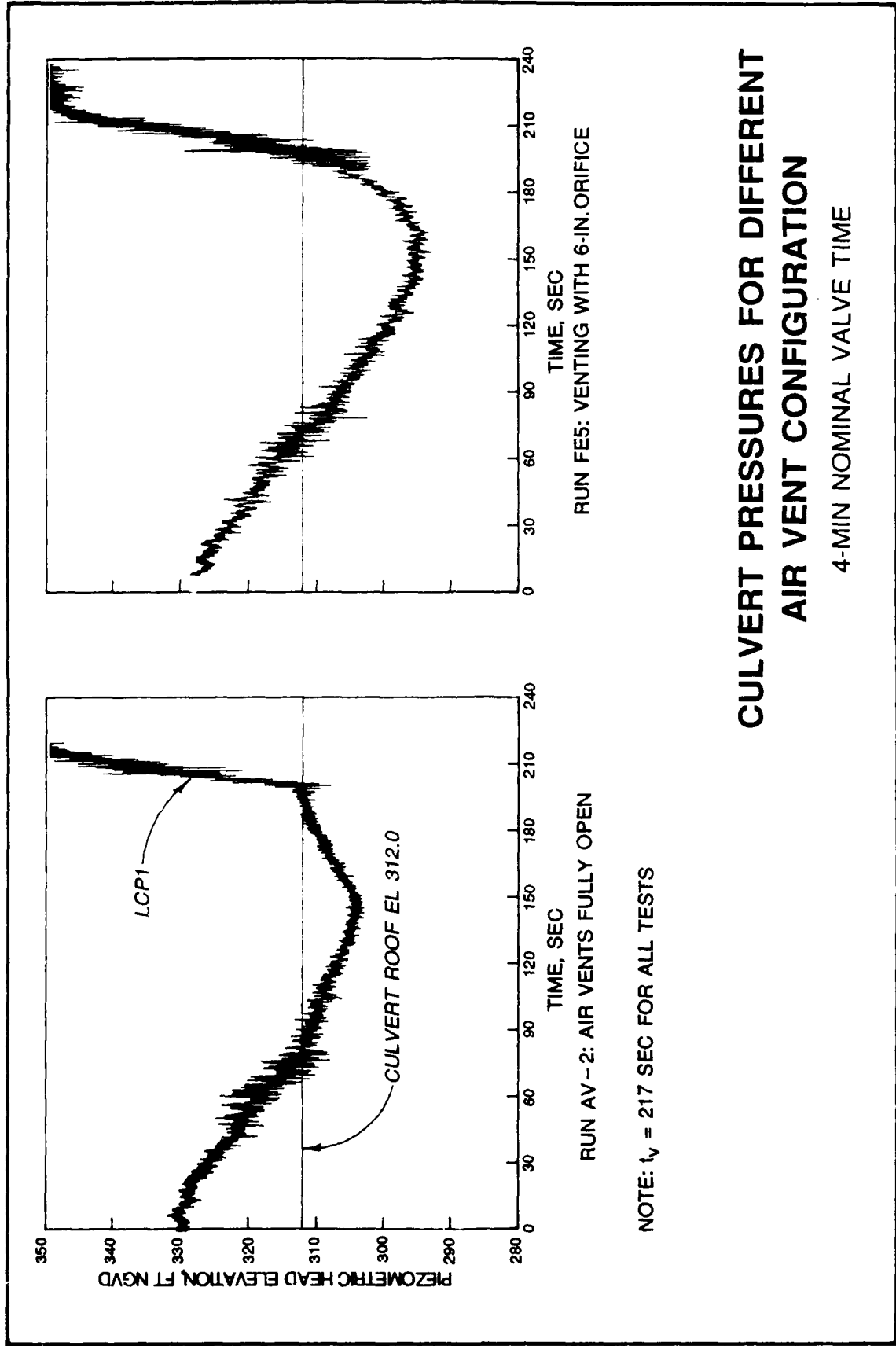


RUN AV-3: AIR VENTS CLOSED

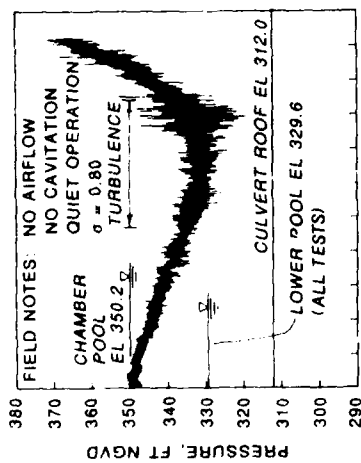
NOTE:  $t_v = 66$  SEC FOR ALL TESTS  
 DATA SAMPLED AT 512 S/S FOR RUNS AV-1, AV-3  
 DATA SAMPLED AT 20 S/S FOR RUN FE7

## CULVERT PRESSURES FOR DIFFERENT AIR VENT CONFIGURATIONS

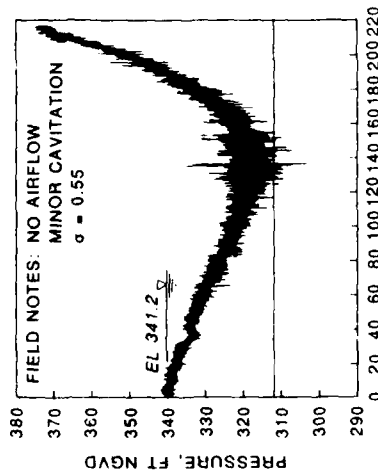
1-MIN NOMINAL VALVE TIME



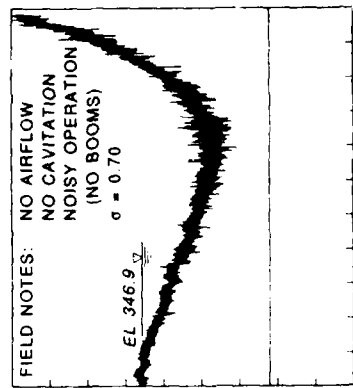
**CULVERT PRESSURES FOR DIFFERENT  
AIR VENT CONFIGURATION**  
4-MIN NOMINAL VALVE TIME



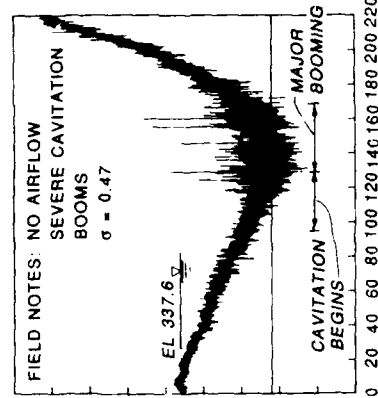
RUN CA1-1



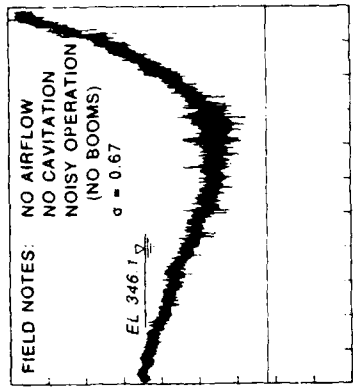
RUN CA1-5



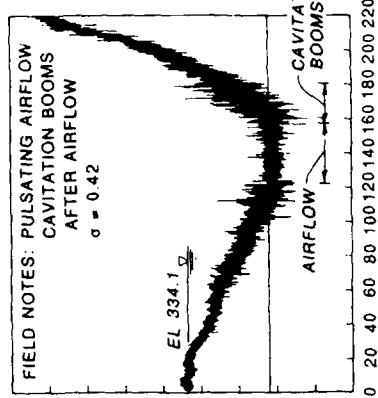
RUN CA1-3



RUN CA1-6



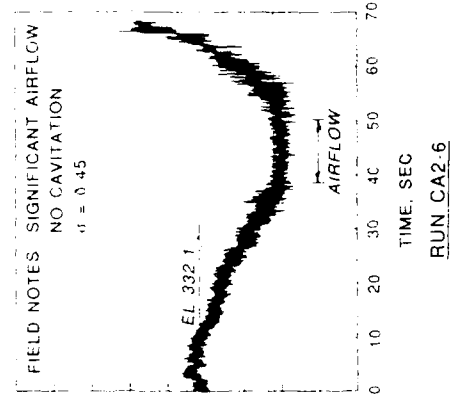
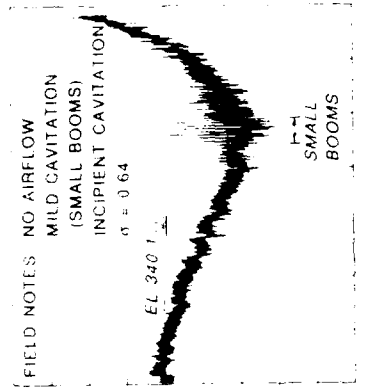
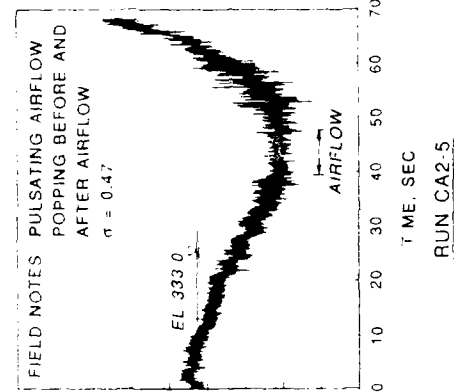
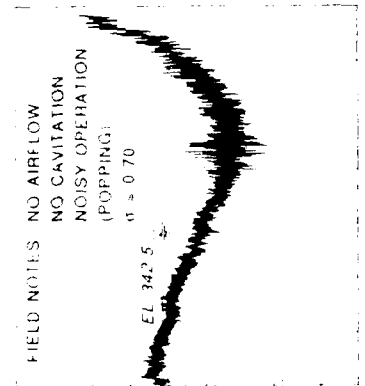
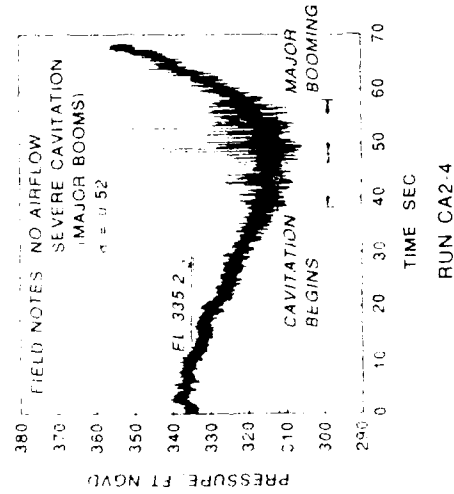
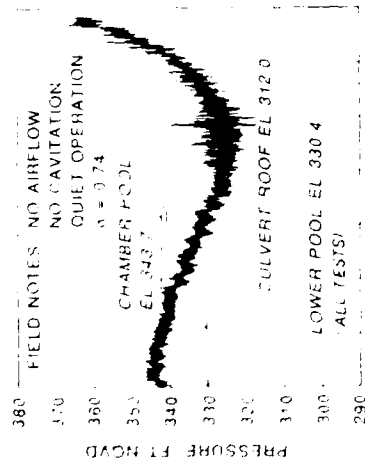
RUN CA1-4



RUN CA1-7

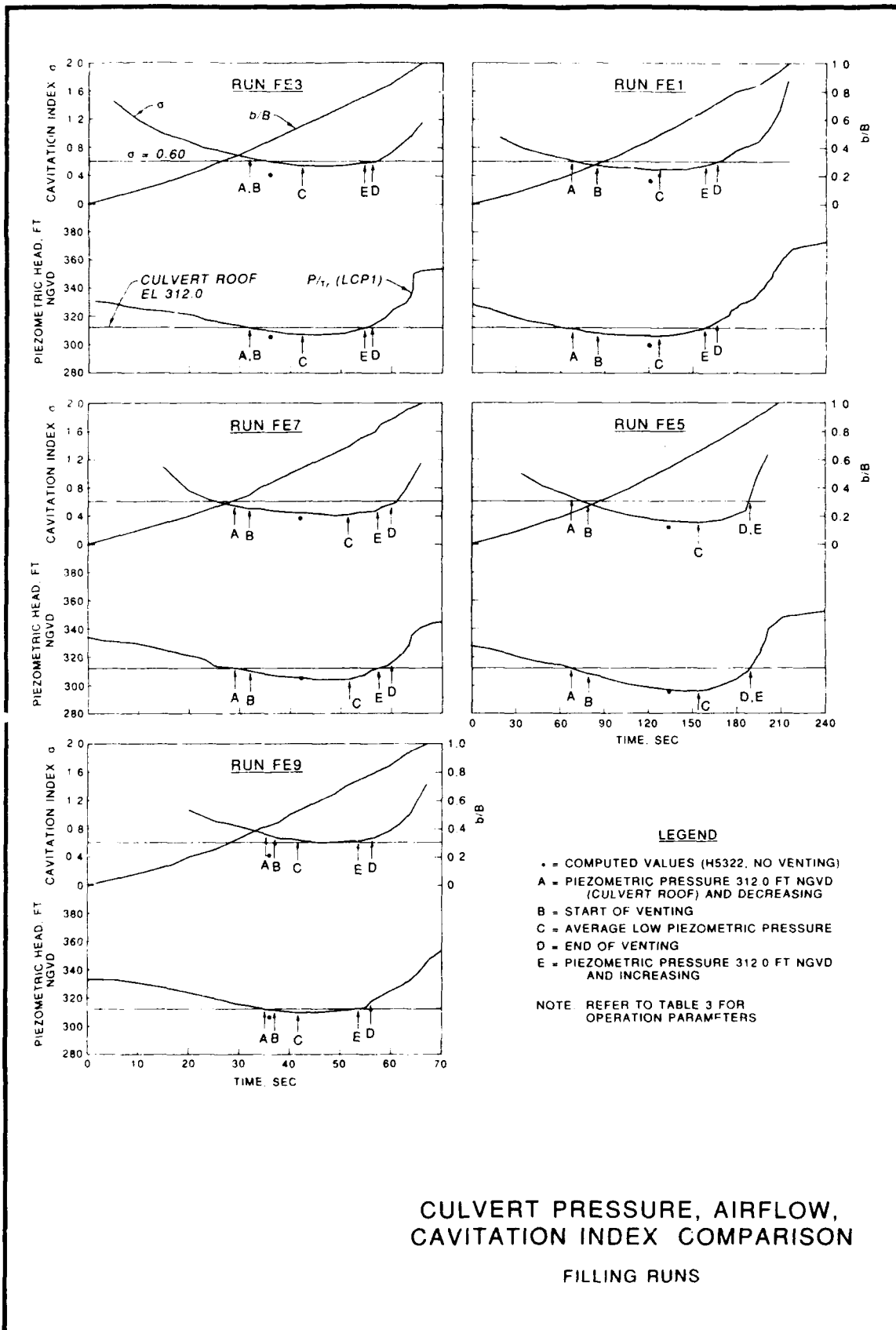
EFFECT OF SUBMERGENCE ON  
CULVERT ROOF PRESSURE DOWNSTREAM  
OF FILLING VALVE  
TWO-VALVE FILLING  
3.63 MIN VALVE RATE

NOTE:  $\sigma$  IS THE MINIMUM COMPUTED BY H5322



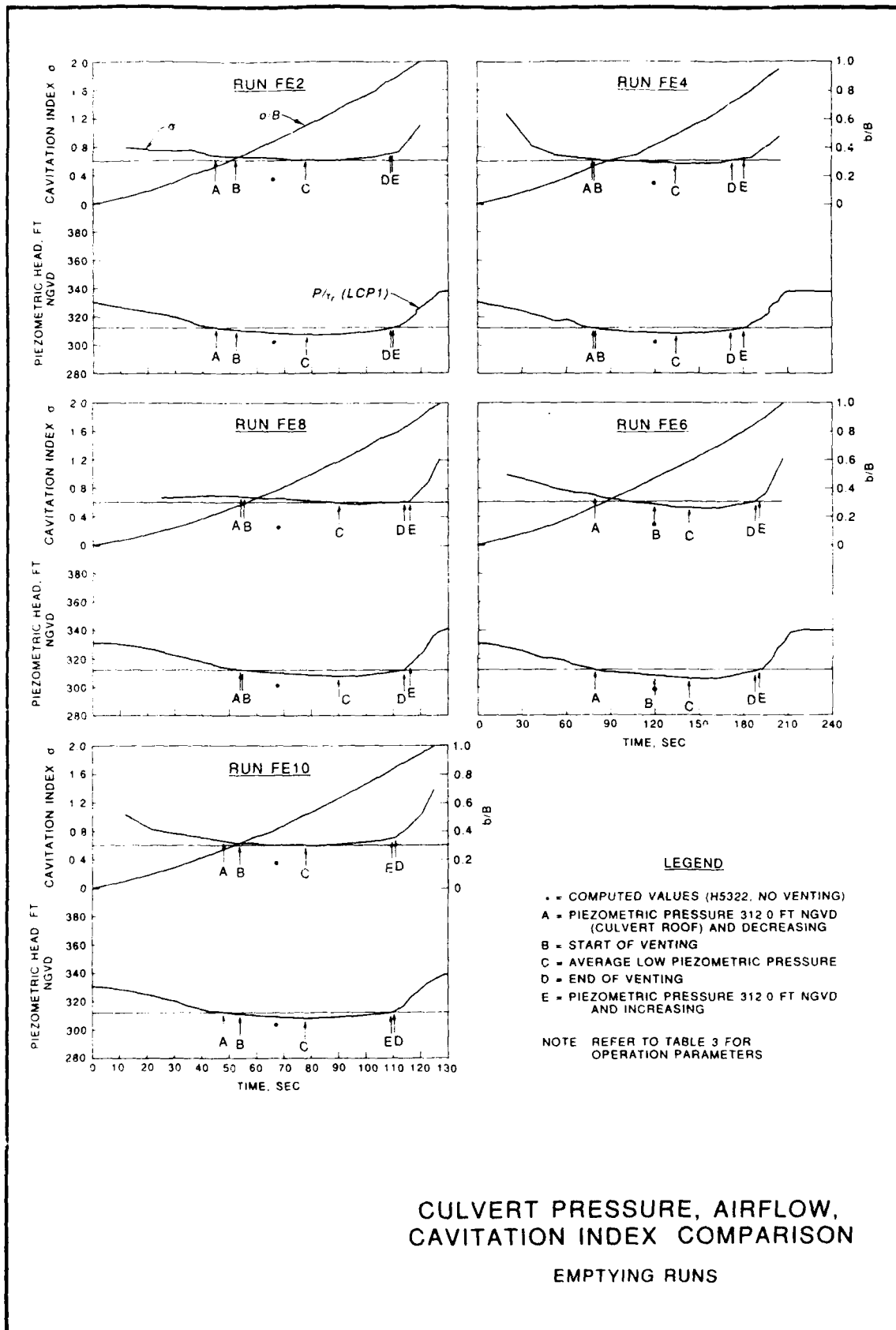
EFFECT OF SUBMERGENCE ON  
CULVERT ROOF PRESSURE DOWNSTREAM  
OF FILLING VALVE  
TWO-VALVE FILLING  
1.1 MIN VALVE RATE

NOTE  $\sigma$  IS THE MINIMUM COMPUTED BY H5322



CULVERT PRESSURE, AIRFLOW,  
CAVITATION INDEX COMPARISON

FILLING RUNS



**CULVERT PRESSURE, AIRFLOW,  
CAVITATION INDEX COMPARISON**

**EMPTYING RUNS**

APPENDIX A: NOTATION

A	Orifice area, in. <sup>2</sup>
A' <sub>c</sub>	Cross-sectional area of culvert
A <sub>i</sub>	Area of conduit i
A <sub>L</sub>	Water-surface area in lock chamber
b	Tainter valve opening (vertical distance between the culvert floor and the valve lip)
B	Maximum valve opening (14 ft)
C	Culvert system discharge coefficient
C <sub>c</sub>	Valve contraction coefficient
C <sub>d</sub>	Valve discharge coefficient; orifice discharge coefficient
C <sub>L</sub>	Lock coefficient
d <sub>e</sub>	Maximum overempty distance
d <sub>f</sub>	Maximum absolute overfill distance
d <sub>o</sub>	Overtravel, ft
dz/dt	Rate of rise of lock water surface
F	Frequency
g	Acceleration of gravity
H	Total head or initial differential head
H <sub>L</sub>	Total head loss
k	Valve coefficient
k <sub>t</sub>	Overall loss coefficient
k <sub>v</sub> , k <sub>1</sub> , k <sub>2</sub> , k <sub>3</sub> , k <sub>4</sub>	Specific loss coefficients (defined in Figure 15)
H <sub>m</sub>	Overall inertial head
L	Length or distance
L <sub>i</sub>	Length of conduit i
L <sub>m</sub>	Inertial length coefficient

n	Number of culverts
p	Pressure
$(p/\gamma_w)_r$	Pressure at culvert roof
Q, $Q_t$	Flow rate
$Q_a$	Air vent flow rate
$Q_w$	Water discharge
r	Subscript denoting roof
$t_e$	Overempty time
$t_f$	Overfill time
$t_m$	Time at which rate of rise of water surface reaches the maximum
$t_v$	Valve opening time
t, $t_1$ , $t_2$	Time (general)
T	Lock operation time
V	Water velocity at the vena contracta, fps
$V_c$	Average velocity of flow in the culvert
y	Water depth at the vena contracta, ft
z	Elevation of water surface in the lock chamber
$Z_r$	Culvert roof elevation
$Z_L$	Lower pool elevation
$Z_U$	Upper pool elevation
$\beta$	Angle of the gate lip
$\gamma_w$	Specific weight of water (62.4 lb/ft <sup>3</sup> at 60° F)
$\Delta H$	Differential piezometric head evaluated across the valve
$\Delta P$	Difference in pressure head immediately upstream and downstream of the orifice, psid
$\rho_a$	Mass density of the air
$\sigma, \sigma_i$	Cavitation parameter (incipient)